DEVELOPMENT OF LINEAR MOTOR FOR VIBRATING SAMPLE MAGNETOMETER

by

Mustafa KOÇ

April 2014

DEVELOPMENT OF LINEAR MOTOR FOR VIBRATING SAMPLE MAGNETOMETER

by

Mustafa KOÇ

A thesis submitted to

the Graduate Institute of Sciences and Engineering

of

Meliksah University

in partial fulfillment of the requirements for the degree of

Master of Science

in

Material Science and Mechanical Engineering

April 2014
Kayseri, Turkey

I certify that this thesis satisfies all the requirements as a thesis for the degree of Master of Science.

Professor M.Halidun KELEŞTEMUR
Head of Material Science and Mechanical Engineering Division

This is to certify that I have read this thesis and that in my opinion it is fully adequate, in scope and quality, as a thesis for the degree of Master of Science.

Assistant Professor A.Esad Özmetin
Supervisor

Examining Committee Members

It is approved that this thesis has been written in compliance with the formatting rules laid down by the Graduate Institute of Sciences and Engineering.

Prof. Dr. Halidun KELEŞTEMUR
Director

April 2014

DEVELOPMENT OF LINEAR MOTOR FOR VIBRATING SAMPLE MAGNETOMETER

Mustafa KOÇ

M.S. Thesis - Materials Science and Mechanical Engineering
April 2014

Supervisor: Asist. Prof. A.Esad Özmetin

ABSTRACT

Since the first explorations of magnetic materials, systems that measures the magnetic properties of materials have been popular in scientific communities. Most commercial products have competed with each other to achieve the most accurate measurements of magnetic properties, therefore a huge marketing potential came out during the recent decades.

In this thesis, a linear motor was designed and manufactured for one of the most effective and fastest magnetic property measurement systems, which is called the Vibrating Sample Magnetometer.

In this study, a motor module that allows for the up and down movement of the sample is designed. Using Maxwell, a linear motor system depending on Lorentz force calculation and optimum magnet-current distances is geometrically analyzed. At the end of the Maxwell analysis, we obtained values that bring us to the best current-force binary of linear motors that have ever been produced for VSM. In the light of the Maxwell analysis, we designed the VSM linear motor head via the Solidworks software package.

Using Solidworks, CAD drawing of the motor and probe were carried out, and in addition, simulations were performed for cases of thermal extension of the materials used. For this reason, essential tolerances for the dimensions of the motor system were determined.

The measurements performed showed that, depending on the quality of the materials that we have used in the motor, especially the bearings, desired motion capabilities could be achieved.

After manufacturing the linear motor through 3 different types of machining, the motion, thermal and vacuum tests were performed and the results are illustrated by their respective curves and figures.

Keywords: Vibrating Sample Magnetometer, Linear Motor, Sinusoidal Oscillation

TİTREŞTİRMELİ ÖRNEK MANYETOMETRESİ İÇİN DOĞRUSAL MOTOR GELİŞTİRİLMESİ

Mustafa KOÇ

Yüksek Lisans Tezi – Malzeme Bilimi ve Makine Mühendisliği
Nisan 2014

Tez Yöneticisi: Yrd. Doç.Dr. Ali Esad Özmetin

ÖZ

Manyetik malzemelerin ilk keşiflerinden beri, malzemelerin manyetik özelliklerini ölçen sistemler bilim dünyasında popüler oldular. Çoğu ticari üretimler manyetik özelliklerin en doğru sonuçlarını verebilmek için birbirleriyle yarıştılar. Böylece son yıllarda büyük bir pazarlama alanı ortaya çıktı.

Bu yüzden manyetik özellikleri ölçen en etkili ve hızlı sistemlerden biri olan Vibrating Sample Magnetometer sistemi için Doğrusal motor bu tezde tasarlanmaya ve üretilmeye çalışıldı.

Numuneyi yukarı ve aşağı hareket ettiren motor modulü tasarlandı. Motor modülü tasarımında, elektromanyetik analiz programı Maxwell‘ den yararlanıldı. Maxwell kullanılarak doğrusal bir motor sistemi, Lorentz kuvveti eşitliği ve optimum akım-mıknatıs mesafeleri baz alınarak, geometrik olarak analiz edildi. Maxwell analizi sonunda daha önce VSM için yapılan doğrusal motorlar içinde en iyi akım-kuvvet çifti değerine ulaşıldı.

Solidworks programı kullanılara, motorun ve sondanın CAD tasarımı yapıldı. Ayrıca, motorda kullanılan malzemelerin ısıl genleşmeleri simule edildi. Bu sebeple motor sistemi içindeki parçaların gerekli mesafe toleransları ayarlandı.

Maxwell analizleri ışığında, Solidworks kullanılarak VSM doğrusal motor kafası tasarlandı. Motor içinde kullandığımız malzeme kalitesine bağlı olarak, özellikle doğrusal rulmanda, isteğimiz hareket değerlerine ulaşabildik.

3 farklı CNC torna makinesiyle üretilen Linear motorun hareket, ısınma ve vakum testleri resimlerle ve grafiklerle kanıtlandı.

Anahtar Kelimeler: Titreştirmeli Örnek Magnetometresi, Doğrusal Motor, Sinüzoidal Titreşim

DEDICATION

Dedicated to my friends, supervisor and family members for their endless support and patience during the forming phase of this thesis.

ACKNOWLEDGEMENT

I thank to Turkish Ministry of Industry, Technology and Science for supporting this thesis under the project number 01277.STZ.2012.1.

I thank to my supervisor Asist. Prof. A. Esad Ozmetin for his helps. He encouraged me to go through this thesis and enlightened me by his knowledge and experience.

In addition, I thank to my friends in our research group, who are Engin YAZICI, Mehmet KURU and Erhan ONGUN for all supports.

I also thank to Nanomagnetic Scientific Instruments and people who works for this company.

Finally, I thank to my patient family to encourage me and trust me.

TABLE OF CONTENTS

LIST OF TABLES

TABLE

LIST OF FIGURES

FIGURE

LIST OF SYSMBOLS AND ABBREVIATIONS

SYSMBOL/ABBREVIATION	
VSM	Vibrating Sample Magnetometer
CNC	Computer Numerical Control
MIT	Massachusetts Institute of Technology
SQUID	Superconducting quantum interference device
AC	Alternative Current
DC	Direct current
C	Celcius
PAR	Princeton Applied Research
emu	Electromagnetic unit
Am^2	Amper square meter
Oe	Oersted
K/minute	Kelvin per minute
RF	Radio frequency
Hz	Hertz
W	Watt
Ω	Ohm
A	Amper
V	Volt
rpm	Revolutions per minute
hp	Horse power
dB	Decibel
CAD	Computer Aided Design
N/m	Newton per meter
T	Tesla

UHV	Ultra high vacuum
Hz/s	Hertz per second
PCB	Printed circuit board
p-p	Peak to peak

CHAPTER 1

INTRODUCTION

1.1.OBJECTIVE OF THESIS

Vibrating sample magnetometer is one of the most useful magnetometer for the measurement of the magnetic properties of magnetic materials. In the global market of magnetic measurement devices, VSM has an important place in the sale of laboratory measurement systems.

Vibrating sample magnetometers (VSM) exhibit high sensitivity, accuracy and reliability along with their simple structure is, which makes them quite useful in laboratories and factories. The main functionalities can be listed follows:

i) Basic magnetic properties (magnetization curve, hysteresis loop, the demagnetization curve, thermal magnetic curve, etc.), ii) To give the corresponding various magnetic parameters (such as the saturation magnetization, residual magnetization, coercive force, the maximum energy product, and the Curie temperature, magnetic permeability (including the initial magnetic permeability), etc.), iii) To measure the magnetic properties of materials composed of powders, granules, film, liquid, block, etc. iv) Situ measurements of magnetic materials from liquid nitrogen temperature up to 500°C temperature zone magnetic variation with temperature curve [1].

It should not be ignored that one of the most important parts in a VSM device is a suitable linear motor having advanced motion characteristics. That’s why, in this study we attempted to design an effective, inexpensive, stable device having less mechanical or magnetic noise electromechanical sample vibrating drive for Vibrating Sample Magnetometer (VSM). Not many drive (motor) designs with these properties have been proposed since the first discovery of the VSM. The first goal is to survey

for the designs in literature in order to find some different types of drivers that have been designed for commercial or academic use in the laboratory. The motor must have a perfect sinusoidal motion in linear direction and a harmony from the top point to the bottom point where the sample is going to be probed. Its amplitude and frequency, at least, have to have optimum necessity for the signal that is proportional to the magnetic moment of the sample. The drive system should have as low mechanical vibration as possible during its operation. The second goal is to validate our own design with the above properties using specialized software packages such as Maxwell and Solidworks and their related components. Third is the manufacturing step in which CNC machining was used to form the parts of the instrument that were designed in Solidworks. Finally, the motor drive system was tested in terms of motion capability and vacuum protection as well as its thermal features by a series of circuits, vacuum pump and thermocouple, respectively. These steps will be explained detail through this text.

1.2. BRIEF HISTORY OF VSM

Early VSMs were described by Blackett (1956), Van Oosterhout (1956) and Foner (1956). These devices were suitable for the detection of magnetic moments induced in samples exposed to external magnetic fields. The first detailed description of a VSM was given by Foner (1956, 1959) and his original design has been a basis for many subsequent VSMs. The first scientific VSM was invented by Simon Foner at Lincoln Laboratory of MIT in 1955 **[**2].

The instrument has been used in several configurations including the original commercial model FM-l unit, which was marketed and most widely used in the 1960s by Princeton Applied Research (PAR) Corporation [3].

Foner published a more detailed paper in 1959, and several other papers that associated with various aspects of this device were published (Flanders and Doyle 1962, Case and Harrington 1966, Mallinson 1966, Foner and McNiff 1968, Springford et al. 1971, Bowden 1972, Foner 1974). These papers concentrated on

the modifications on the original Foner design, discussion of the coil arrangements or sensitivity considerations[4]. Van Oosterhout, Plotkin, and Flanders used a similar instrument but differing from Foner's vertically vibrated sample, they vibrated the sample in the direction of the field [5].

Many types of magnetometers have been developed and are now commercially available. Today's VSM devices may have different structures, however, they are based on same principle.

These instruments have been thoroughly reviewed by Foner and can be classified into two major categories: (i) Some were employed as direct techniques, such as measurement of the force experienced by the specimen in a non-uniform field (Guoy, Faraday, Kahn balances); (ii) Others were based on indirect techniques such as measurement of magnetic induction due to relative motion between the sample and the detection coils system (vibrating sample, vibrating coil, SQUIDs) or use of galvanomagnetic effects such as the Hall effect. The vibrating sample magnetometer (VSM) has been proved to be most efficient for low temperature and high magnetic field studies of correlated electron systems due to its simplicity, robustness, ease of measurement and reasonably high sensitivity [5].

A hysteresis loop shows the relationship between the induced magnetic flux density (B) and the magnetizing force (H). It is often referred to as the B-H loop. The hysteresis loop parameters can be listed the Saturation magnetisation (Ms), Coercive field (He), Remanence (M) and Squareness ratio (M/Ms). A sample hysteresis curve for a vibrating sample magnetometer (VSM) is given in Figure 1.1 [6].

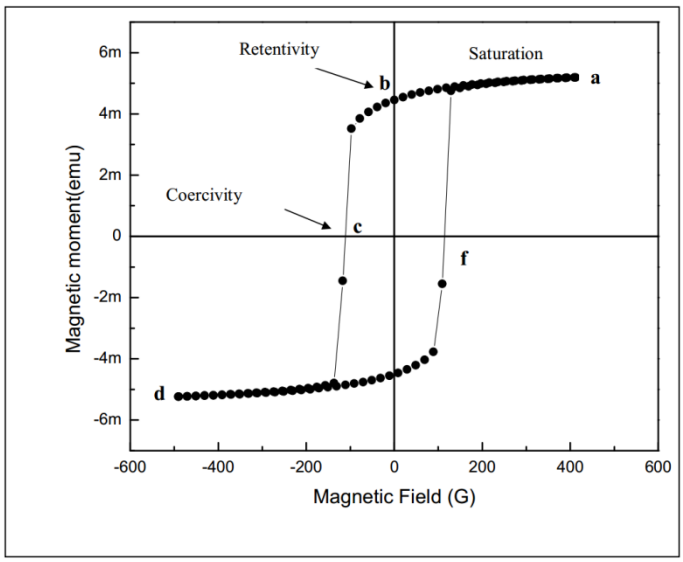

Figure 1.1 : An example hysteresis curve of a Fe film [6].

Various types of magnetic property studies are reported in literature for different materials including paramagnetic, ferromagnetic, antiferromagnetic, diamagnetic and ferrimagnetic. VSM's have been used in the study of amorphous and magnetic bubble domain materials, and also the nature of the bonds in intermetallic components has been investigated. Additionally, the studies have included the measurement of the hysteresis loops of magnetic tape and disc materials and the rare earth compounds. Finally, the VSM is ideal for superconductivity measurements (Meissner effect, diamagnetic shielding, and critical field determination) and the study of the magnetic properties of thin films or single crystals [7].

CHAPTER 2

WORKING PRINCIPLE OF VSM

2.1. THEORETICAL DESCRIPTION OF VSM

In a VSM, a sample of interest is placed in a constant magnetic field. If the sample is magnetic, this constant magnetic field will induce a magnetization on the sample through aligning the magnetic domains or the magnetic spins along with the field. The magnetic dipole moment of the sample will create a magnetic field around the sample, which is termed the magnetic stray field. In a VSM, the sample undergoes sinusoidal motion which induces an electrical signal in the pick-up coils according to the Faraday's law of induction. This signal is linearly related to the magnetic moment of the sample, the amplitude of vibration and frequency of the signal. The magnetometer separates other signals from that of the magnetic moment of the sample to obtain the net magnetic moment. The VSM consists of a head assembly for the sinusoidal motion of the drive, the sample rod, electromagnet assembly, controller and a computer. The transducer in the head assembly, which may be,a loud speaker, converts a sinusoidal AC drive signal to a vertical vibration of the sample rod. The sample is normally placed at the other end of the rod which is placed in between the poles of an electromagnet. The coils mounted on the pole pieces of the electromagnet pick up the signal resulted from the sample motion. A vibrating capacitor beneath the transducer generates an AC control signal proportional to the vibrational amplitude and frequency, or most of the advanced systems use encoder to create this signal. This signal is fed back to the oscillator where it is compared with the drive signal and also it is phase-adjusted and routed to the signal demodulator where it functions as the reference drive signal. The signal from the sample is also buffered, amplified and applied to the demodulator. There, it is demodulated with respect to the reference

signal from the moving capacitor assembly. The resulting signal gives the sample's magnetic moment alone. For a specific field strength, the corresponding signal received from the probe is translated into a value of magnetic moment of the sample. The voltage change is directly proportional to the magnetic moment of the sample. The various components mentioned in the previous chapter are interfaced via a computer through controlling and monitoring software. A cryogenic setup attached to the sample permits low temperature measurements. A lower limit for measurable magnetic moment around a few $10^{-9}\mathrm{Am}^2(10^{-6}\mathrm{emu})$ can be achieved in commercial setups. The upper limit for measurable moment can be in the order of 1 Am^2 and higher (note that the magnetic moment of a 5 mm diameter iron sphere is nearly 0,1 Am^2) [8].

The basic principle of operation for a vibrating sample magnetometer is that a changing magnetic flux will induce a voltage in a pickup coil. The time-dependent induced voltage is given by the following equation:

$$V_{coiI} = \frac{d\phi}{dt} = \left(\frac{d\phi}{dz}\right)\left(\frac{dz}{dt}\right) \tag{2.1}$$

In equation (2.1), Φ is the magnetic flux enclosed by the pickup coil, z is the vertical position of the sample with respect to the coil, and t is time. For the sinusoidal oscillation of a sample, the voltage can be expressed by the following equation:

$$V_{Coil} = 2\pi f C m A \sin(2\pi f t) \tag{2.2}$$

The acquisition of magnetic moment measurements involves measuring the coefficient of the sinusoidal voltage response from the detection coil [9].

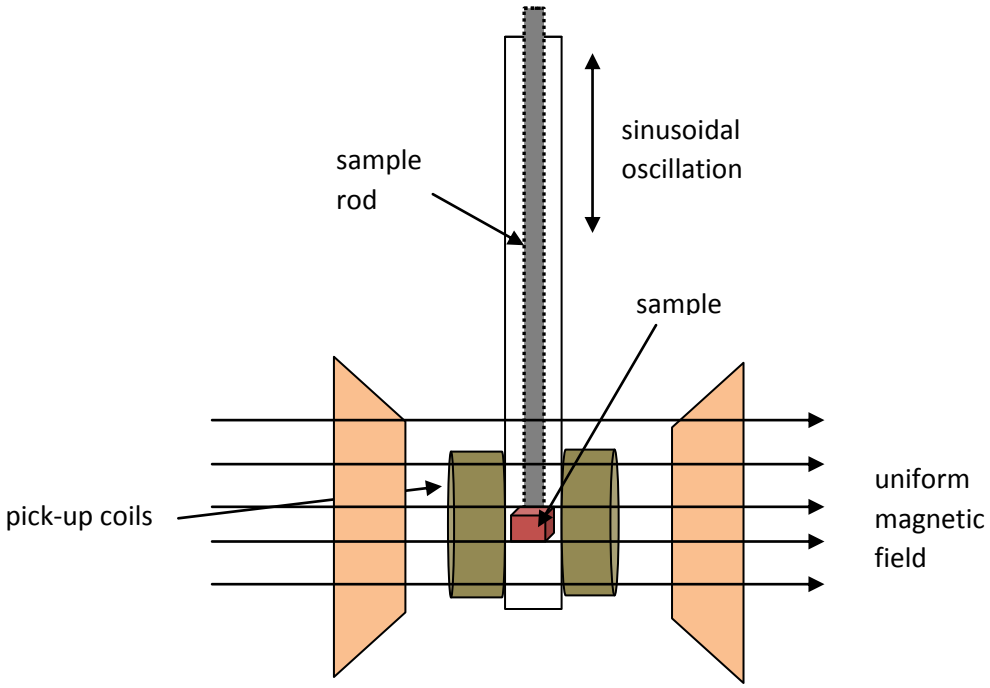

Figure 2.1 : Schematic representation of VSM.

Another means for sensing the magnetic moment is to use a Hall effect sensor. The following figure indicates the location and geometry of the Hall sensor in the VSM. The Hall effect sensor is a semiconductor device with a current flowing through it. When a magnetic field penetrates the sensor at 90º to its surface, a voltage is induced perpendicular to the current path (Figure 2.2). This voltage varies approximately linearly with field strength.

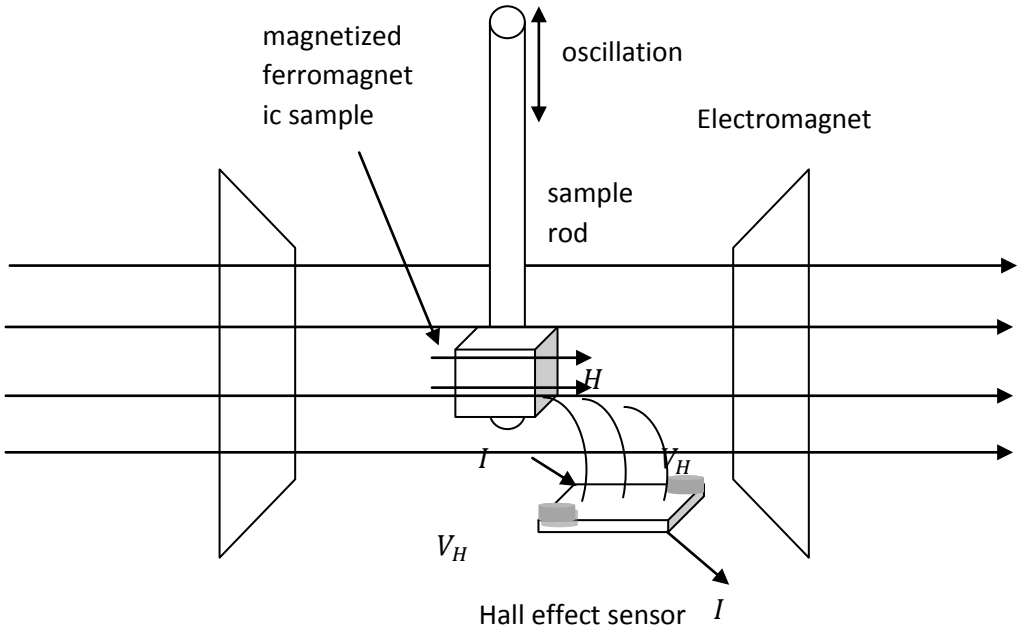

Figure 2.2 : Working principle of Hall sensor (element) in VSM.

As the sample rod oscillates, the ferromagnetic sample will be magnetized and a component of its field will enter the sensor that results in a Hall voltage. Equations to find the magnetic moment of the sample using Hall effect are as follows;

$$V_H = \frac{M \gamma I_c \, d \sin(wt)}{2} \tag{2.3}$$

where M: Magnetization detected Am^{-1}, γ : Hall sensitivity $VI^{-1}A^{-1}m$, I_c: Current through Hall sensor(element) I, d: Amplitude of oscillation m, w: Angular frequency of sample oscillation s^{-1}

$$\gamma = \frac{V_H}{IH} \tag{2.4}$$

where V_H: Voltage from the Hall sensor V, I: Current through the Hall sensor I, H : Magnetic field perpendicular to Hall surface Am^{-1}. Rearranging to find the magnetization and removing the oscillating term which is removed by the lock-in amplifier yields [10].

$$M = \frac{2V_H}{dI_c \gamma} \tag{2.5}$$

2.2. GENERAL STEPS OF MAGNETIC PROPERTY MEASUREMENT

A typical measurement on a sample can be taken in the following manner:

1. The strength of the constant magnetic field is set
2. The sample begins to vibrate
3. Measuring absolute position of a target mechanically coupled to sample using a position sensor or an encoder
4. Resolving the output of the position sensor into an AC component and a DC component
5. Using independent AC and DC feedback loops responsive to AC and DC components, respectively, to control the vibration or oscillation of the sample
6. The signal received from the probe is converted into a value for the magnetic moment of the sample
7. The strength of the constant magnetic field is changed to a new value. No data is taken during this transition
8. The strength of the constant magnetic field reaches its new value
9. The signal from the probe again is converted into a value for the magnetization of the sample
10. The constant magnetic field varies over a given range, and a plot of magnetization (M) versus magnetic field strength (H) is generated
11. The VSM measures the difference of magnetic induction between one region of space with the sample and another without the sample, thus allowing calculation of the magnetic moment, m, generally with a sensitivity in the order of 10^{-5} emu [10].

CHAPTER 3

NECESSITY OF ULTRA LOW VIBRATION AND NOISE

3.1. EFFECTS OF NOISE ON VSM MEASUREMENTS

The maximum sensitivity of the VSM can be achieved by using an extremely stable and homogenous magnetic field. In the case of any field instability or external vibrations of coils placed in a non-homogenous field may be selected by the detection coils, therefore reducing the sensitivity of magnetization measurements.

Any background constant flux is automatically filtered and signal optimization can be pursued if some degree of flexibility exists in term of the amplitude and frequency of the oscillation and the arrangement of the sensing coils. A popular VSM operates based on this principle.

The main goal of a high-sensitivity magnetic moment measuring device is not only the perfect characterization of permanent magnets and recording media, but also suitable for weakly magnetic and paramagnetic materials [11].

Since the first publication of the description of a VSM, there have been a considerable number of publications that present the improvements in any aspects of the instrument. In general, the quality of a VSM measurement depends on the proper integration of all components of the VSM, namely the sample drive, pick-up coils, magnetic field generation, and signal detection electronics [12].

One main concern of the whole apparatus was noise and several measures were taken for the reduction of it.

Since the work of S. Foner, the most difficult problem in VSMs has been vibrating the sample without friction and avoiding mechanical coupling between the vibrator and the detection coils, which leads to noisy signals. The improvements to these systems were described as high sensitivity, very good field and temperature accuracy, and a wide temperature range.

The vibrator without the sample rod operates in a way such that the voltage induced in the pickup coils is very small and constant. However, with the sample rod involved, a noisy signal that increases as being weakly dependent on the field and temperature, is observed, which arises essentially from the mechanical coupling between the vibrator and the pickup coils due to the sample rod. This noisy signal can be removed from the measurements, and for that purpose, measurements versus field are performed without the sample at ten different temperatures. A fit of each isotherm is made using a polynomial expansion to the fifth order. The rod correction at any temperature is obtained by linear interpolation. Synchronism enables sophisticated phase sensitive detection of very small signals that would otherwise be swamped by noise [13].

Many VSM systems, including Quantum Design Inc., determine common sources of measurement error in VSMs. In general, the following sources of background signal and noise are expected.

3.1.1 Magnetic Field Errors:

The reported magnetic field is derived from the net current that is passing through the magnet solenoid. However, the actual magnetic field at the sample location may differ from the reported magnetic field due to the magnetic flux trapped inside the solenoid. This trapped flux occurs because electrical currents may indefinitely wander within the superconducting wire which lacks electrical resistance, and, in turn, generate a remanent magnetic field. This magnetic field error depends on

the recent history of the magnet and is usually the most problematic when the reported magnetic field is very low, or zero.

To reduce the magnetic field errors, a known paramagnetic reference must be used to determine the remanent field and the data can be post-processed to correct for this error, if necessary. Automating the magnet charging with a sequence to create a reproducible magnet history helps make the remanent field reproducible for a given series of measurements. The remanent field will be different if different charging operations are utilized to set the same magnetic field. The remanent magnetic field should be characterized following each magnet charging operation in our sequence [13].

3.1.2. Sample Holder Errors:

Lake Shore Cryotronics, Inc. offers a number of related issues that may have effect the efficiency of a VSM in conducting magnetic measurements on low moment materials.

First, VSM measurements on low moment samples will often be affected by the diamagnetic or paramagnetic contributions arising from the sample holder: and in the case of thin films, the film substrate material. To extract the magnetic signal coming from the magnetic layer, background signals requires: minimization of the sample holders magnetic signature, and a means for subtracting the substrate contributions.

Sample holders developed and characterized by very small magnetic signals are optimal for low moment measurements. Moreover, a substrate material must be measured and subsequently subtracted from the film + substrate data yielding the magnetic signal from the magnetic layer, or a linear correction must be applied to the film + substrate data to analytically remove substrate contributions.

In the Figure 3.1, the contribution from noise sources in the hysteresis loop for a CoCrPtTa alloy HD film sample (5 mm × 5 mm) is shown. VSM head mounting can be used to isolate the VSM head from the electromagnet and sensing coils, thus eliminating head vibration coupling and improving the linearity of the background signals and VSM sensitivity.

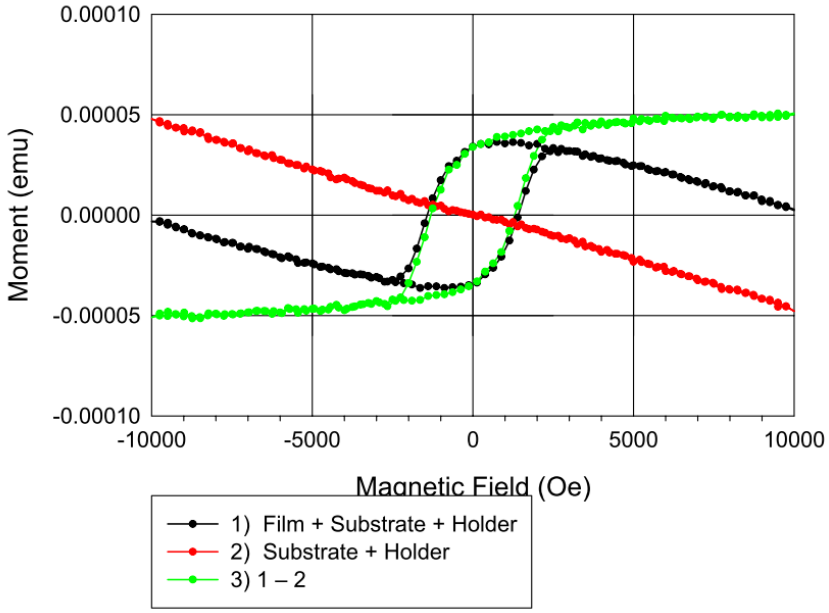

Figure 3.1: Hysteresis M(H) loops for a CoCrPtTa alloy HD film sample (5 mm × 5 mm)[14].

Data were recorded at ambient temperature and for applied fields of 10 kOe (1 T) aligned in-plane and parallel to the easy axis of magnetization. Data are presented for: 1) Film + substrate + holder, 2) substrate + holder, and 3) (1) – (2), or the M(H) loop for the magnetic film only. Note that at very low background signal arises from the VSM sample holder. Even with the diamagnetic substrate, contribution to the total signal is only 50 μemu at 10 kOe [14].

3.1.3. Sample Location Errors:

Improperly-located samples will yield measurement errors. It is important to determine the correct sample offset before beginning the measurements. If the

sample temperature will be changed during or between measurements, it is important to adjust the sample location during the measurement process. Thermal contraction of the sample rod and the sample holder will result in a change in the location of the sample.

In order for the elimination of Sample Location Errors, using the auto-tracking feature is the best way to automatically adjust the sample location. When utilizing the periodic centering scan option, instead, the sample location might not be adjusted for each reading, and noticeable jump discontinuities may appear in the data each time the sample location is adjusted.

3.1.4. Loosely Mounted Samples:

When the samples are not mounted securely to the sample holder they will not undergo smooth sinusoidal motion within the detection coils. The sample signal will be rejected as unknown measurement behavior and the sample may potentially be defeated to the sample holder and become lost. Therefore, it is very important to mount samples securely for accurate measurements.

To eliminate the errors caused by loosely mounting, sample may be held in place on the sample holder in a variety of ways: screw clamps, various forms of springs clips, or adhesives. The magnetic properties of the sample mounting materials need to be carefully considered, and usually background measurements are a necessity.

3.1.5. Temperature Errors:

The sweep rate of the temperature will dictate the accuracy of the reported temperature as compared to the actual sample temperature. The analytical function should provide reasonable accuracy for sweep rates up to 10 K/minute. It is always advantageous to report the actual sample temperature, not just the thermometer

reading. However, for higher sweep rates, the user should validate the accuracy by comparison to a known response, like the Curie-Weiss behavior of dysprosium oxide.

3.1.6. Environmental Sources of Noise:

The VSM system can be sensitive to environmental sources of noise. The most troublesome cause of such noise is the broadband RF radiation associated with arc welding or RF-induction sources. Electrical transformers are also a possible source of noise. There are indications that cell phones can also disrupt the VSM signal. Another concern is stray magnetic fields associated with charging of other magnets.

For the rejection of environmental errors, noise-induced errors, the full shield around the dewar will help decrease these effects. A simple technique to determine whether the system takes noise from external noise sources is to monitor the VSM voltage as a function of time. Discontinuous changes must be looked for in the VSM voltage. While it is best to isolate and remove the sources of noise, the VSM lock-in style measurement and other software features may be able to reject this noise as well [14].

3.1.7. Vibration of Pick-up coil:

The signal in the pick-up coils is typically very small (the signal caused by a few nano-Volts) and therefore extremely sensitive to noise sources. The pickup coils themselves must be mechanically isolated from the vibrating source since vibration of the coils relative to the field may give an additional error in the voltage at the measuring frequency. A trans-impedance amplifier and a lock-in amplifier are therefore used to extract the small magnetic signal from the sample. One of the major causes of problems in such a system are vibrations of the coils relative to the field applied by the electromagnet. The flux produced by the magnetic sample is approximately 10^{-15}times smaller than the flux produced by the magnet, and

therefore, vibrations must be canceled by the same factor. Development of this type of instrument is a multidisciplinary task that involves electrical, physical, and mechanical aspects.

The signal generated in the pickup coils of the VSM depends on several factors:

1. the number of turns in each coil as well as the coil orientation and geometry,
2. the amplitude and frequency of the sample vibration
3. the size of the magnetic moment, M and volume of the sample, V.

Factors 1 and 2 are instrumental parameters that can be identified by calibration. The size of the magneti moment depends on the sample volume and its magnetization density, which is a function of field and temperature by turns. So the VSM signal depends on the state of magnetization of the sample, M, through H and T. The VSM output is a plot of M vs. H at a constant temperature of special interest, or M vs. T at a constant field.

Fake signals can be induced in the coils if they vibrate in the applied field, and these signals are not only too high, but may also be slightly non-homogeneous. Vibrations are principally caused by mechanical coupling between the vibrating assembly and the coils. They introduce a significant problem because the ensuing signal that has the same frequency as the signal induced by the vibrating sample, cannot be filtered out by the lock-in amplifier.

The easiest way of minimizing the effect of pick-up coil vibrations may be locking the coils to the magnet. An additional measure consists of placing vibration dampers or even active anti-vibration elements between the vibrating head and the rest of the apparatus [15].

An additional factor to the ones mentioned so far is the Johnson noise generated in the coils. Johnson noise, in general terms, is the random variation of voltage due to the thermal agitation of charge carriers in a resistor. A review of several sensitivity issues has been given in H.J.Richter 1992 (H. J. Richter, J. Magn. Magn. Mater. 111, 201(1992)). This might be due to a more stable electromagnet power supply. If

proper cabling, impedance matching, and amplification is used, the system noise can be brought back close to (within 2–3x) the theoretical limit presented by the electrical (Johnson) noise. The Johnson noise is given by $\sqrt{4kTR\Delta f}$, where R is the sensor impedance and Δf is the effective noise bandwidth of the signal amplifier. A few thousand turns of small diameter copper wire (0.1 mm or less) are normally used in each coil, which implies a resistance R around 100 Ω and higher. Johnson nois has a white spectrum of density $\Phi(f) = 4kTR$, with k being the Boltzmann's constant and T the absolute temperature. If the measurement bandwidth is Δf, the associated r.m.s, voltage is $V_{rms} = 4kTR\Delta f$ [16].

3.1.8. Type of Sample

In case of thin films or hard disks, the contribution from the substrate can be larger than the contribution from the magnetic material. In case of error from thin film subtrate, it must be subtracted by making measurements with and without the magnetic layer [17].

3.1.9. Vibrating System Errors

There exists another type of vibration that can be caused by a mechanical coupling between the vibrator and the detection coil system or by other sources of vibration around the VSM. The detection coil system is highly sensitive to flux changes in order to be able to measure the small flux changes caused by the sample motion. Therefore, vibrations of the detection coils (which change the angle between the detection coil axes and the magnetic field or move the coils in the slightly inhomogeneous applied field) will also cause flux changes in the detection coils, depending on the field strength. To this end, the vibrating head is supplied by a reference signal generated by the lock-in amplifier and suitably amplified. Mechanical and electrical effects may cause a drift in the performance of the vibrator. For this reason, a reference signal can be generated in a pair of coils by a permanent magnetor by an encoder attached to the vibrating rod at a distant position

from the measuring pickup coils, it is amplified and compared by software to the target signal.

There are no special restrictions as to the frequency of vibration, provided it is far from any mechanical resonance frequency of the apparatus. Since frequency and amplitude of the vibration go hand-in-hand, it is required that products guarantee useful signal amplitude [17].

Two other common ways to reduce this problem are the use of vibration dampers between actuator and measurement system and a rigid coupling of the detection coils to the magnet. A disadvantage of commonly used vibration dampers in or directly attached to the vibrator system, is that because of the low mass of the damped system and the low frequency of the vibrations, the damping materials must be very compliant. As a result, the whole vibrator–sample holder assembly can move freely, which gives rise to a poor definition of the exact sample position [18].

In order to prevent this, the vibrator unit can be mounted on a heavy table (Figure 3.3), which can be damped by much stiffer vibration dampers, so that the sample positioning remains reliable. A third way of vibration damping is the use of passive or active anti-vibration elements. Some commercial systems like the Princeton Applied Research (PAR) and Oxford Instruments VSMs utilize passive spring mounted weights which, if properly tuned, will vibrate in anti-phase to the actuator and therewith can significantly reduce the induced vibrations in the system. In order to overcome this, an active system is used in some systems. This type incorporates a second actuator driving a dummy mass mounted on top of the first actuator and driven at the same frequency but with amplitude and phase tuned such that the vibrations in the system can be reduced, if vibration feedback is used [19]. Both the vibration isolation elements and the anti-phase vibration system are shown in Figure 3.2.

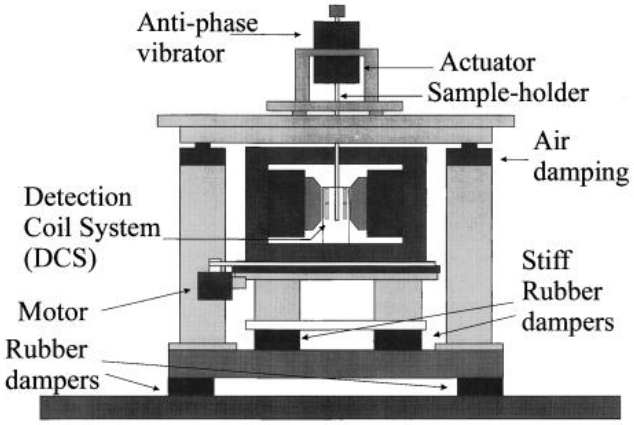

Figure 3.2: Schematic of the VSM setup including anti-phase vibrator and vibration damping[19]

Figure 3.3 : Heavy vibration damper by air on the Cryogenic system, which being used by our research group.

CHAPTER 4

NECESSITY OF A SINUSOIDAL MOTION

If the sample vibrates with sinusoidal motion a sinusoidal electrical signal can be induced in suitably placed pick-up coils. The signal will have the same frequency of vibration and its amplitude will be proportional to the magnetic moment, amplitude, and relative position with respect to the pick-up coil system. In case of hitches like non-sinusoidal motion of the sample, which can possibly occur during the measurement, measurement errors can be developed [20].

4.1. REASONS AND EFFECTS OF NON-SINUSOIDAL MOTION

4.1.1 Overview of Non-Sinusoidal Motion of the Sample

The sinusoidal vibration of the sample causes the magnetic flux through a nearby pick-up coil to vary sinusoidally. A voltage is induced in the pick-up coils, which is proportional to the magnetization of the sample [21].

A common example of Quantum Design, Inc. also determines a non-sinusoidal vibration which causes some noise in the VSM measurement is that;

Precise VSM measurements require smooth sinusoidal motion of the sample within the pickup coils. Deviations from this ideal motion will produce artifacts in the measured magnetic moment of the sample. This may occur in the following cases:

i. A sample is not fixed tightly in the sample holder and subsequently rattles.
ii. A powdered sample is not packed tightly and the material shakes within the sample holder.

iii. A glue or screw joint on the sample rod is loose so that the sample holder slips.

iv. The most important one is the case of vibrating mechanism errors which include poor feedback to the linear motor or linear motor defects, and the mechanical frictions and manufacturing defects in a mechanical crank system, if used, that prevent an exact sinusoidal motion is to be achieved.

Figure 4.1 shows magnetic moment vs. temperature data from a nickel sphere. Its behavior is noisy and erratic, based on the following observations:

i. The moment data exhibits significant noise and jumps.

ii. The quadrature signal "M Quad. Signal", which describes any moment pickup that is not in phase with the expected signal based on the motion of the motor, is a significant fraction (~5%) of the moment signal.

iii. The standard error "M. Std. Err.", which describes the uncertainty in the reported moment value, exhibits large scatter.

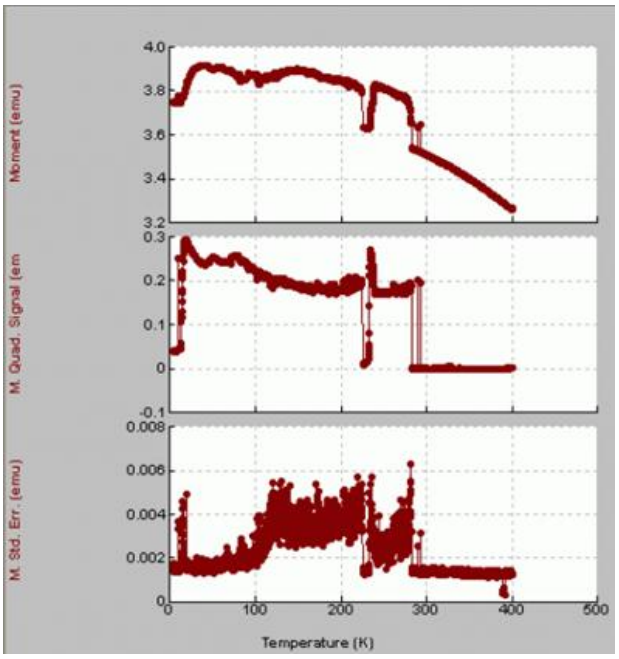

Figure 4.1. Magnetization vs. temperature data for nickel, with sample rattling in the sample holder below 290 K [22]

In contrast, at temperatures above 300 K the moment data is smooth, and the quadrature signal and standard error are both less than 0.5% of the sample moment.

The noisy data is explained by the fact that the sample was not moving sinusoidally with the motor, but was instead rattling around in the sample holder. A significant quadrature component arose because the loose sample lagged behind the motion of the motor.

The explanation of the noise appearing only at temperatures below 290 K can be made by the loose joints between parts originating from the differantial thermal contraction of materials [22].

The AC signal which is induced by the sinusoidal vibration frequency of the sample is proportional to the magnitude of the moment of the sample. However, since it is also proportional to the vibration amplitude and frequency, the moment readings taken simply by measuring the amplitude of the signal are subject to errors due to variations in the amplitude and frequency of vibration.

In order to avoid this difficulty, a nulling technique is frequently employed to obtain moment readings that are free of these sources of error. These techniques make use of a vibrating capacitor or an encoder for generating a reference signal that varies with moment, vibration amplitude, and vibration frequency in the same manner as the signal from the pickup coils. When these two signals are processed in an appropriate manner, it is possible to eliminate the effects of vibration amplitude and frequency shifts. In that case, one obtains readings that vary only with the moment of the sample [23].

4.1.2 Effect of the Vibration Amplitude and Frequency:

The amplifier is locked to just the vibration frequency, and ignores signals of other frequencies; this permits the detection of very small signals which would

otherwise be lost in background noise. This locking requires a good precision mechanical vibration and mechanical vibration system, accordingly.

The sample signal scales linearly with the vibration amplitude. Therefore, changing the vibration amplitude is an effective way to scale the signal when it is too large or too small. Vibration amplitude can be increased if the sample does not generate a large enough signal, and decreasing the amplitude could be a good action if the sample generates too large a signal. The instrument accounts for this signal dependence so that the reported moment remains accurate when the vibrating amplitude is changed. Since the vibration amplitude range of the instrument is effective at only one order of magnitude (0.5 mm – 8.0 mm), this technique yields two orders of magnitude in the instrument's dynamic range for magnetic measurements.

Although a default vibration frequency corresponds to a mechanically quiet frequency for a VSM system as a whole. There is little reason to use any different vibration frequency. In fact, by using a different frequency one may undesirably detect additional noise due to electromagnetic or mechanical resonances in the instrument or within a laboratory. If a laboratory contains a source of noise, it is useful to change the vibration frequency of the VSM. The AC power in the laboratory (usually 50 Hz or 60 Hz) is the most predominant source of erroneous signal for instruments such as the VSM. When using a different vibration frequency it is recommended to verify measurement accuracy using another the supplied material reference [24].

CHAPTER 5

SAMPLE DRIVE SYSTEMS

5.1. PREVIOUSLY MANUFACTURED SAMPLE DRIVES

The drive systems may be a voice coil drive, a linear stepper motor, a piezolelectric transducer, a pneumatic system, a mechanic crank system etc. One of the most widely used driving systems in VSMs; the voice coil actuators are direct drive, limited motion devices that utilize a permanent magnet field and coil winding(conductor) to produce a force that is proportional to current applied to the coil. These electromagnetic devices are orginally used in loudspeakers and create a basis for loudspeaker motion sources.

There must be a condition for monitoring and/or controlling the amplitude as well as the frequency of vibration. Control of the AC drive amplitude using an AC feedback signal has become standart procedure to maintain precise control of sample oscillation. VSM is very sensitive to sample motion [25].

While much work has been done in the past, there are a number of shortcomings of existing drive technologies. For example, current mechanical assemblies used in a VSM drive can require warming times of several hours to achieve stability. Furthermore, such assemblies can show drifts associated with enviromental changes such as temperature and humidity. Also, any non-linearities in the AC behaviour of the feedback sensor can cause variations in the VSM output.

5.1.1. Electromechanical Drive (Linear Motors and Voice Coils) Systems

Electromagnetic conversion mechanism of a voice coil actuator is governed by the Lorents Force Principle. If a current-carrying conductor is placed in a magnetic field, a force, F will act upon it. Magnitude of this force is determined by the magnetic flux density, B, the current, I, and the orientation of the field and current vector. Furthermore, if a total of N conductors (in series) of lenght L are placed in magnetic field, the force acts on those conductors is shown by equation:

$$F = kBLIN \tag{5.1}$$

where k is a constant. As shown in Figure 5.1, the direction of the force generated is a function of the direction of current and magnetic field vectors. Specifically, it is the cross-product of the two vectors. If current flow is reversed, the direction of the force on the conductor will also be reversed. If the magnetic field and the conductor lenght are constant, then the generated force is directly proportional to the input current [26].

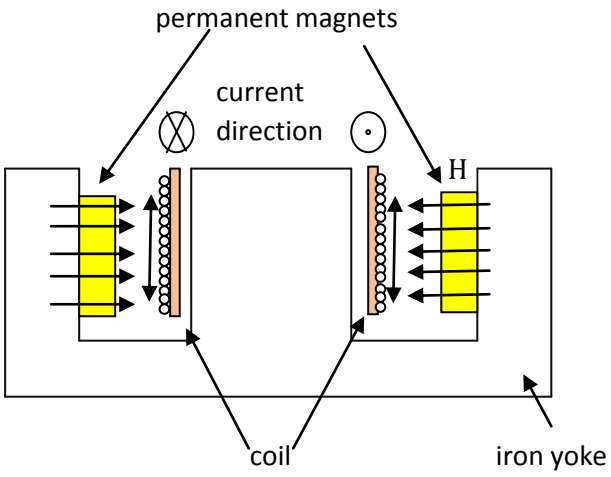

Figure 5.1: Conventional linear voice coil actuator (Loudspeaker) .

In its simplest form, a linear voice coil actuator is a tubular coil of wire settled within a radially oriented magnetic field, as shown Figure 5.1. Most of the VSM manifacturers depend on the principles governing these devices.

The field is produced by permanent magnets embedded on the inside diameter of a ferromagnetic cylinder, arranged so that the magnets that are face-to-face with the coil are all of the same polarity. An inner core of ferromagnetic materials set along the axial centerline of the coil, joined at one end to the permanent magnet assembly, is used to complete the magnetic circuit. The force generated axially upon the coil when current flows through the coil will produce relative motion between the field assembly and the coil, provided the force is large enough to overcome friction, inertia, and any other forces from loads attached to the coil.

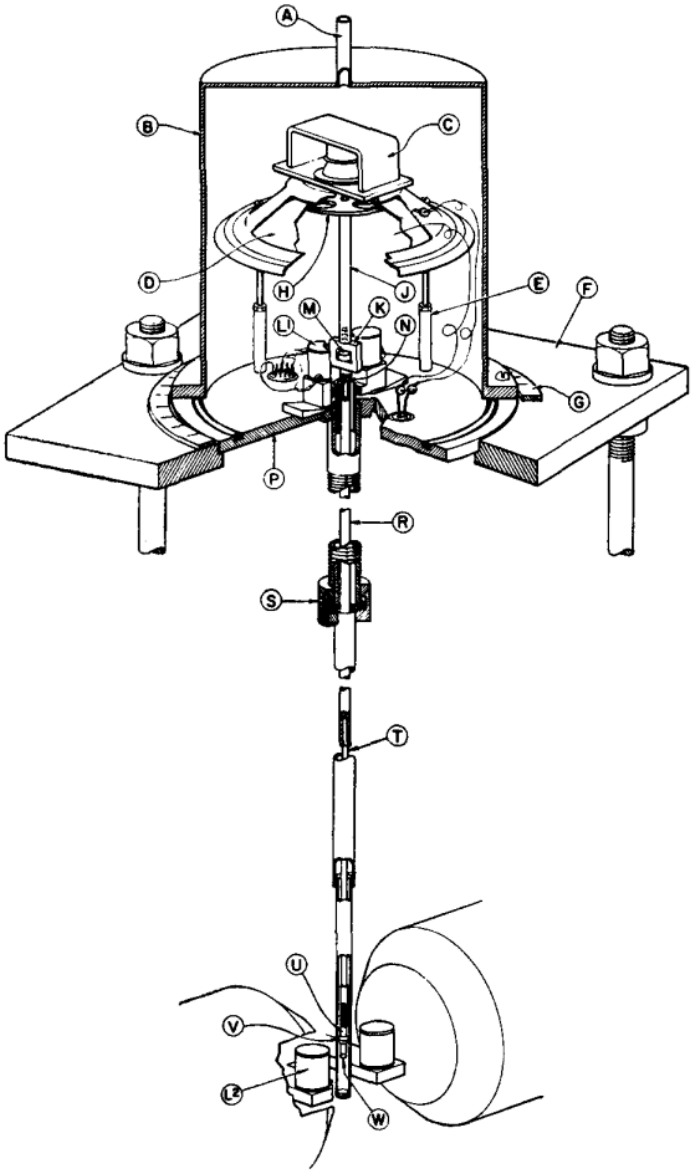

Figure 5.2: First generation vibrating sample magnetometer design by Foner [27].

Loud speaker design, which is one of the first designs by Foner is illustrated in Figure 5.2. This VSM sample drive uses a feedback sensor that provides not only AC amplitude information on the sample movement, but also absolute position information. This feedback is used in proportional/integral (PI) control loops to control both a DC and an AC drive to the voice coil. The DC drive signal maintains precise positioning of the voice coil/feedback sensor arrangement while the AC drive signal provides the control required for the oscillatory motion of the sample [27].

As in the original Princeton Applied Research FM-1 (PAR) design, the FM-l vibration head unit is used to drive the sample rod at 82 Hz to vibrate the sample under test and produce the sample signal.

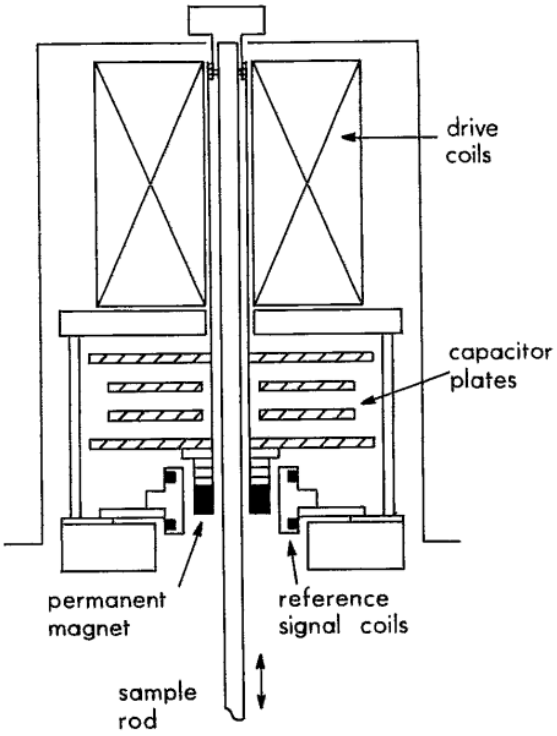

Figure 5.3: Diagram of the Princeton Applied Research FM-1 vibrating sample magnetometer drive head [28].

For the present purposes, it was desired to have a reference signal which has a high amplitude and is proportional to the drive amplitude, similar to the original Foner system. The essential features of this arrangement are shown schematically in Figure 5.3 [28].

In one of the first vibration system studies by A. Niazi et al., there are an in-house designed and constructed sample vibrator and associated electronic circuit built to fulfill the following principal requirements; (i) Pure sinusoidal vibrations of

constant frequency; (ii) Stability of vibration amplitude under load variation and friction; (iii) Stable reference signal phase for lock-in detection of the signal.

For the electrodynamic vibrator, they used two Bolton TM mid-range audio speakers (30 W/8 Ω , 12 cm cone) available at the market.

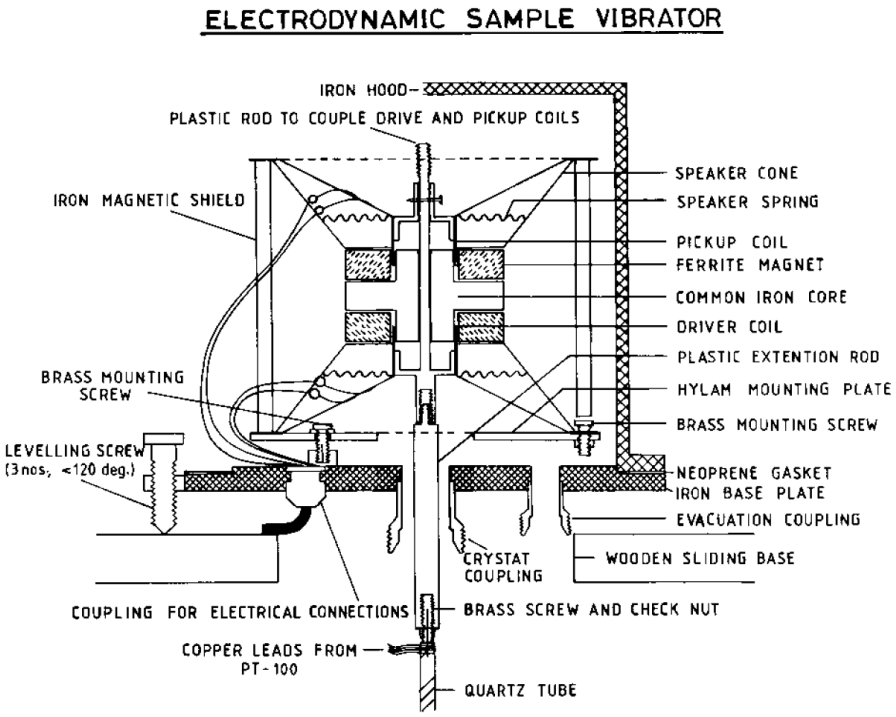

Figure 5.4: Schematic of the electrodynamic sample vibrator (Loud speaker) [29].

The speaker cone and coil sections were glued to their respective ferrite cores so that the two speakers were mounted back-to-back (Figure 5.4). It is necessary that the vibrations of the coil during its operation are not transferred to the base plate and thence to the cryostat and detection coils. Hence, they used anti-vibration mountings. In this arrangement, one of the coils of the vibrator is used as a drive coil for sample vibration while the other acts as a velocity-sensing coil. The signal from the sensing coil is used for negative feedback in order to achieve better stability of sample vibrations [29].

For a physics course in Wesley Burgei et al. the sample oscillation was provided by a Pasco Scientific Model SF-9324 mechanical drive (Figure 5.5) that was mounted to an x–y–z translator. The sample can be fastened with either vacuum grease or a small piece of Parafilm, the latter was used in our case since the small pole pieces and wide gap produced significant field gradients tending to move the sample. To correct for the small variations in vibration amplitude and frequency with time, a reference coil and magnet are often used in research-grade investigations, but they are not employed in the present apparatus.

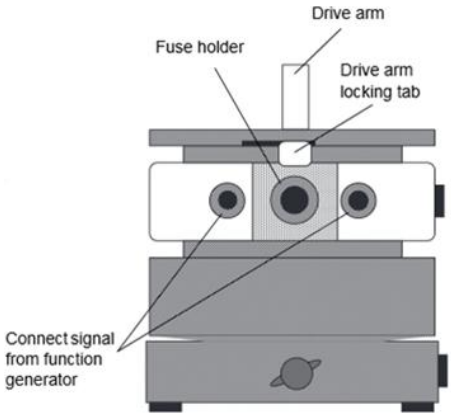

Figure 5.5 : Mechanical Wave Driver, SF-9324 of Pasco [30].

Its frequency response is from 0.1 to 5000 Hz with an amplitude of approximately 3 mm up to about 50 Hz. It requires a function generator with a minimum of ±8 V, 0.5 A in Figure 5.5 [30].

5.1.2. Mechanical (Crank) Drive Systems

In Flanderst and Graham (1993), a synchronous electric motor has sufficient frequency stability and power to produce constant amplitude oscillations up to 1 cm, independent of load. An appropriate synchronous motor (typically 1800 rpm and 1/20hp), a belt and pair of pulleys, and a cam offset, a low-frequency, high-

amplitude vibrating drive (5 Hz, 15 cm) or higher frequency and lower amplitude (100Hz, 0.15 cm) can be construct as in Figure 5.6. A reference signal at the oscillation frequency is needed for the lock-in amplifier.

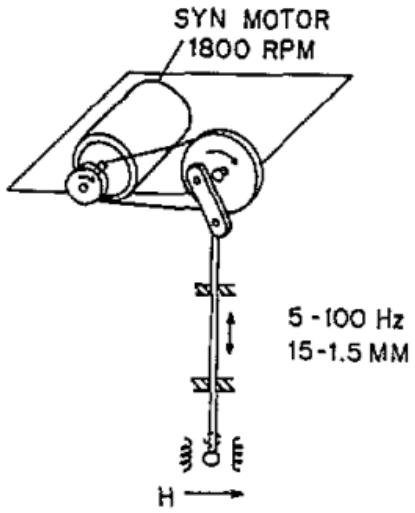

Figure 5.6. Motor drive of Flander & GrahamVSM [31].

They are however, often criticised as being mechanically noisy, although this is usually the result of inadequate balancing and poor mechanical isolation problems. All crank-driven VSM inherently drive the sample in a manner which departs from pure sinusoidal motion [31-32].

Noakes et al (1968) and Redfield and Moleski (1972) have, for example, described motor and crank arrangements. Springford et a1 (1971). Hoon (1983) and most commercial designs have used electromechanical 'loudspeaker' transducers, whilst Mangum and Thornton (1970) have employed a piezoelectric bimorph suitable for the vibration of small sample masses in confined volumes. Piezoelectric gives high vibration frequency but very very low amplitude [33].

In Nizhankovskii et al, the motion was produced by a motor with a crank transducer as was proposed 35 years ago by Johansson and Nielsen.

According to study of Johansson and Nielsen, microcontroller-driven step motor results in ideal constancy of the amplitude and the frequency of the motion. Besides, the step motor was controlled in such a way that the signal from the pick-up coils is perfectly sinusoidal even if the amplitude of the sample motion is comparable with the distance between the coils. A block diagram of the device is shown in following figure.

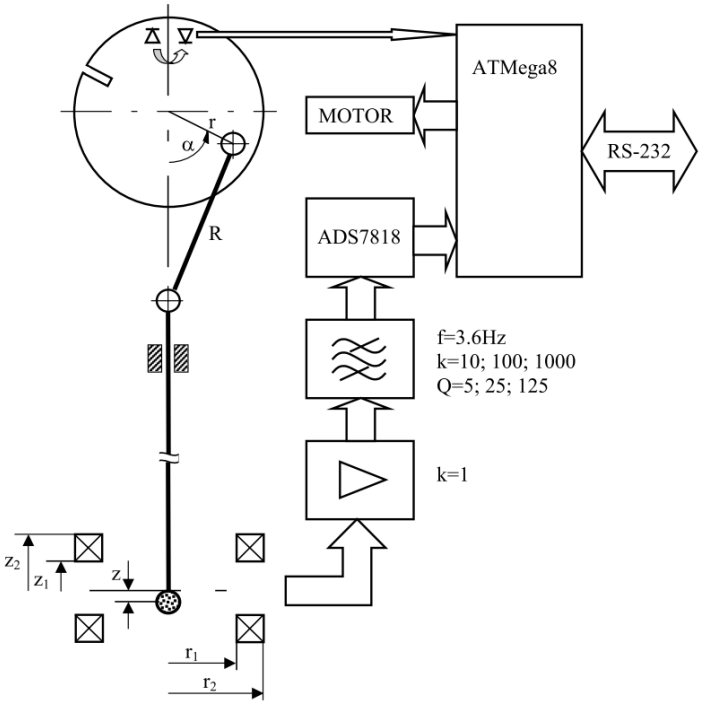

Figure 5.7: Block diagram of a magnetometer with a microcontroller-driven step motor [33].

The upper end of the crank arm R was connected to a crank pin shifted from the motor axis at a distance r. In theory, the sample position as a function of the angle of rotor rotation has the form

$$z(\alpha) = r\cos\alpha + \sqrt{R^2 - (r\sin\alpha)^2} - R + z_0 \qquad (5.2)$$

where z_0 is an inaccuracy in the sample positioning relative to the median plane of the pick-up coils. After a number of calculation, the signal from the pick-up coils is determined as

$$U(t) = \frac{\mu_0 N m_z r}{2s} F(\alpha) \sin\alpha \frac{\mathrm{d}\alpha}{\mathrm{d}t} \tag{5.3}$$

As seen from (5.3) the output signal is non-sinusoidal as a function of time if the step motor rotates with a constant angular velocity. This situation is adverse to further signal processing, in particular to its narrow-band amplification and lock-in detection. The extent of the output signal being non-sinusoidal is determined by two factors.

Firstly, the axial displacement of the sample is non-sinusoidal. There are some formulation causes of this. One has to change the motor rotation speed (in other words the duration of each step) in such a way that the output signal is strictly sinusoidal. It means to be obtained the following condition,

$$F(\alpha) \sin\alpha \frac{\mathrm{d}\alpha}{\mathrm{d}t} = A \sin wt \tag{5.4}$$

where A is the amplitude and ω is the angular frequency of the output signal. It is easy to obtain from (5.4) a connection between the rotation angle α and the time t. The measuring ranges of the magnetometer were 40, 4 and 0.4 emu. The low frequency of sample motion permited them to avoid mechanical problems due to vibration.

Although no additional calibration of the device was needed, an important drawback of this instrument was very low measurement sensitivity due to mechanics limitations [34].

5.1.3 Other Drive Sytems

K.M.Creer et al., Vibration mechanisms have been constructed using a compressed air turbine (Figure 5.8(a)). Rotation was converted to translation by a

scotch crank system which causes the sample to move with simple harmonic motion of large amplitude (1 stroke = 1.2 cm).

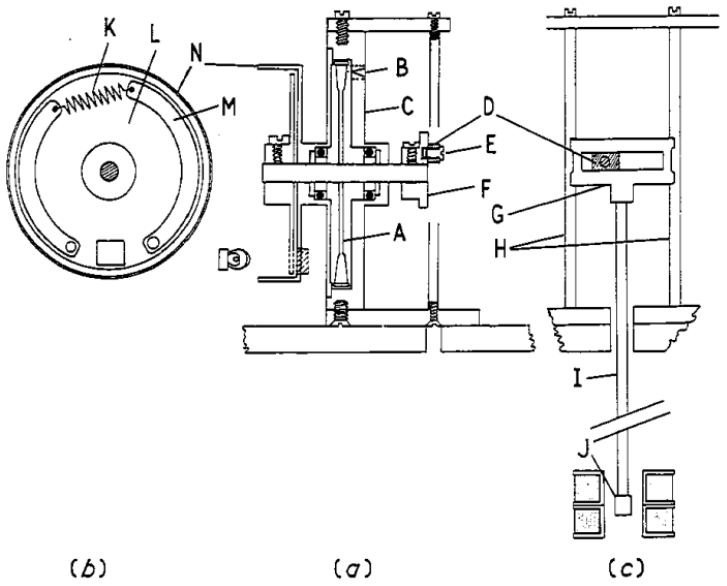

Figure 5.8. Vibration mechanism. (a) Turbine; (b) governor; (c) crank system (for explanation see text) [35].

The scotch crank system (Figure 5.8(c)) is free to rotate about the crank pin. The frequency of rotation was governed by a simple centrifugal brake (Figure 5.8(b)). The friction generated counteracts the low torque of the turbine. The frequency at which the brake was coming into action can be varied by adjusting the position of the fixed end of the spring. The vibrating rod was also made of quartz.

Vibration frequencies up to about 100 Hz could be obtained with an input air pressure of about 1 kg cm^{-2} and a frequency variation of less than ± 0.5 Hz. The operating frequency was set at about 70 Hz. However, it was difficult to perform such extent air pressure easily [35].

In 1982, J.A.Gerber et al studied on a simple vibrating sample magnetometer. The electromechanical drive (G) was a Ling model 203 shaker (Figure 5.10). The sample was able to vibrate at 35 Hz. The shaker and drive rod were coupled via a point contact.

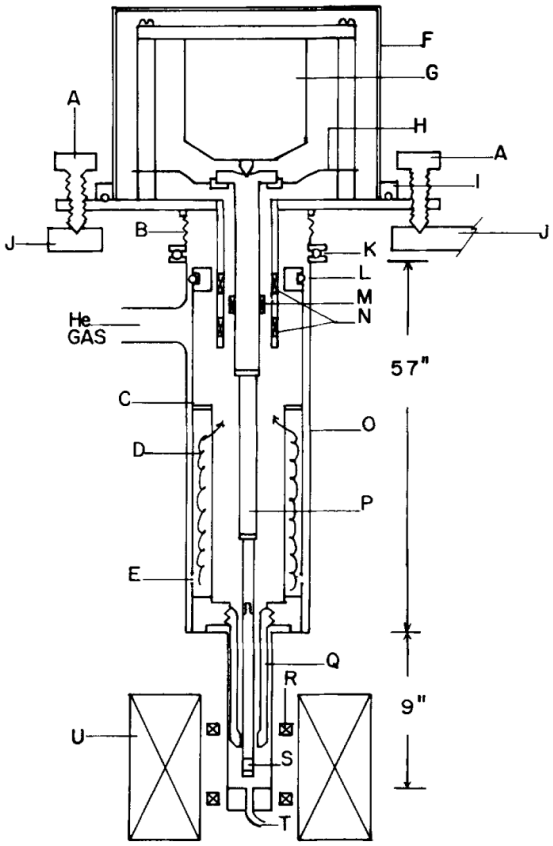

Figure 5.9: Cross section of inner Dewar and inserts [37].

Figure 5.10 : Ling model 203 shaker [36].

Useful resonance range of the shaker is 5-13000 Hz and Max. displacement is 5 mm. It does not allow them to move with more stroke although frequency is enough. It also has 75 dBA acustic noise.

In this system, they had magnetic moment sensitivity of about 10^{-5}emu at zero field and 10^{-4}emu at 80 kOe [37].

5.2. COMMERCIALLY AVAILABLE VIBRATION DRIVE SYSTEMS

In Oct.7,2003, a product was patented. Its assignee was Lake Shore Cry.,Inc. This design is still used by Lake Shore in their design. To mention about this linear drive;

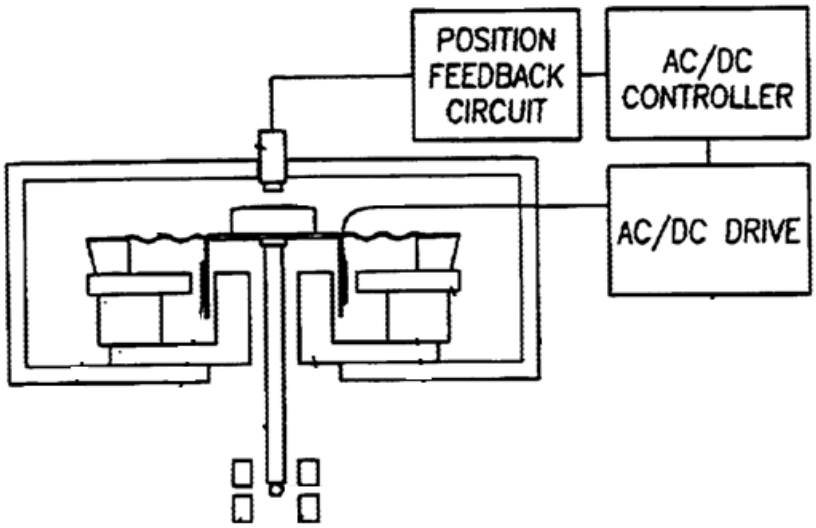

Figure 5.11**:** Schematic illustration of an illustrative exemplary voice coil drive apparatus with pick-up coil [38]

According to them, the apparatus of this invention provided several functional features. First, the AC voltage control was maintaining constant AC vibration amplitude. This was desirable for a good VSM measurement. Second, the DC voltage

control was maintaining the relative position of the coil. This DC provides for increased VSM stabiliy.

In an uncontrolled system, variations in the relative position of the components used in the motion feedback scheme can result from temperature to other environmental changes, resulting in signal drifts and changes in sensitivity of the VSM. For example, in the voice coil drive shown in Figure 5.11, differential thermal expansion of the physical components could cause a shift in the relative position of the eddy currrent sensor. If the feedback system could not detect whether the motion is non-linear, a shift in the sample oscillation amplitude would be directly translated into a shift in the VSM output.

A change in mass changes the loading on the flexible suspension, which alters the positioning of the target. The additional mass also changes the response of the vibrating assembly to the drive signal. With no DC control, a moment variation of 1.19% was observed with a 9.3 gram change in sample rod mass. With DC control, a moment variation of only 0.17% was observed with the same mass change.

As the rod vibrates, the voltage induced in the pick-up coils by the vibrating permanent magnet was used in a feedback loop to control the sample drive. Operating frequencies for the VSM voice coil drives typical take part in the range of 30 to 100 Hertz(Hz) [38].

In present Quantum Design Inc., magnetometers, the VSM linear motor used on PPMS, DynaCool and VersaLab systems typically oscillates at a frequency of 40 Hz, and the sample response was detected at this same frequency. The VSM linear motor, however, is capable of operating over a very wide range of frequencies from 10 Hz up to 80 Hz. During the design of the VSM option, it was found that 40 Hz offered the optimal performance with high sensitivity and low parasitic noise. The parasitic noise was due to vibration of the sample rod which causes a synchronous pickup signal in the coil set when operating in large magnetic fields. While the sensitivity was increasing linearly with frequency, the parasitic noise (which is proportional to the force in the vibration) was increasing quadratically with frequency.

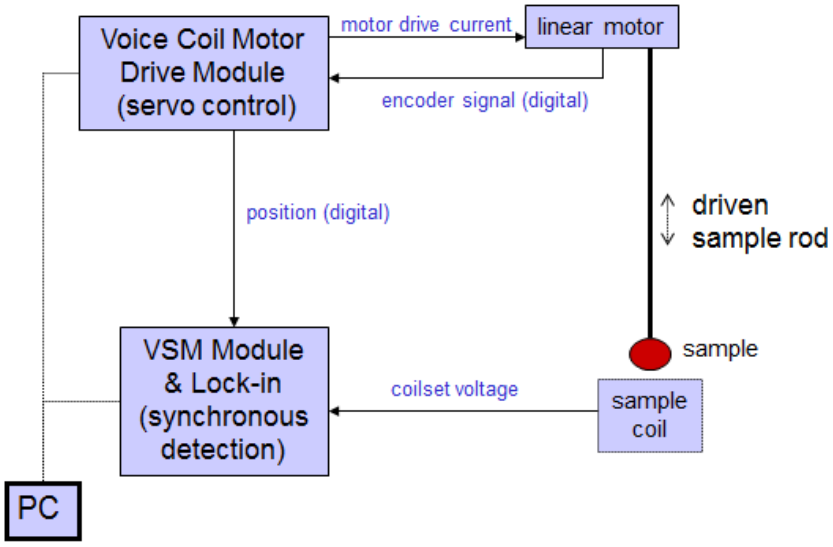

Figure 5.12: Simple VSM block diagram of Quantum Design Inc [37].

The Quantum Design VSM linear motor transport uses linear motor to vibrate the sample (Figure 5.12). The VSM linear motor was designed to operate at 40 Hz, with rapid slewing possible over about 6.5cm (2.5inch) of travel. The large range of motion enables the VSM system to perform rapid. Due to completely automated centering operations, manual adjustments to center the sample will not be needed.

Calculated effect of radial offset for cylindrical samples of different sizes, using oscillation amplitudes of 1 mm and 2 mm. Note that when the centering error is only 1 mm there could be as much as 1% error in the repeated moment.

The Model CM-A VSM motor module is programmed to oscillate the sample at the center of the coilset at a predetermined frequency and amplitude.

Sample centering is one of works of the linear drive has to do properly. Some troubles with centering process that Quantum Design also have some troubles worried when the other chamber problems enter as well. The VSM motor position is fixed at the top of the sample chamber. Thus, the centering of the VSM sample will be affected by relative length changes in the sample chamber versus the VSM sample rod. The VSM software provides a sample centering mechanism.

Figure 5.13 shows a VSM data file for a moment vs. temperature sweep in which sample centering was performed every 10 K or 10 minutes. The “Center Position (mm)” quantity refers to the motor’s position where 65 mm is the top of travel and 0 mm is the bottom, thus any changes to this value will reflect relative length changes between the sample rod and sample chamber.

The main point in this figure is that the sample position is moving for 4 hours after temperature is stabilized at the VSM coil set. This is because of the large thermal mass of the middle portion of the stainless steel tube.

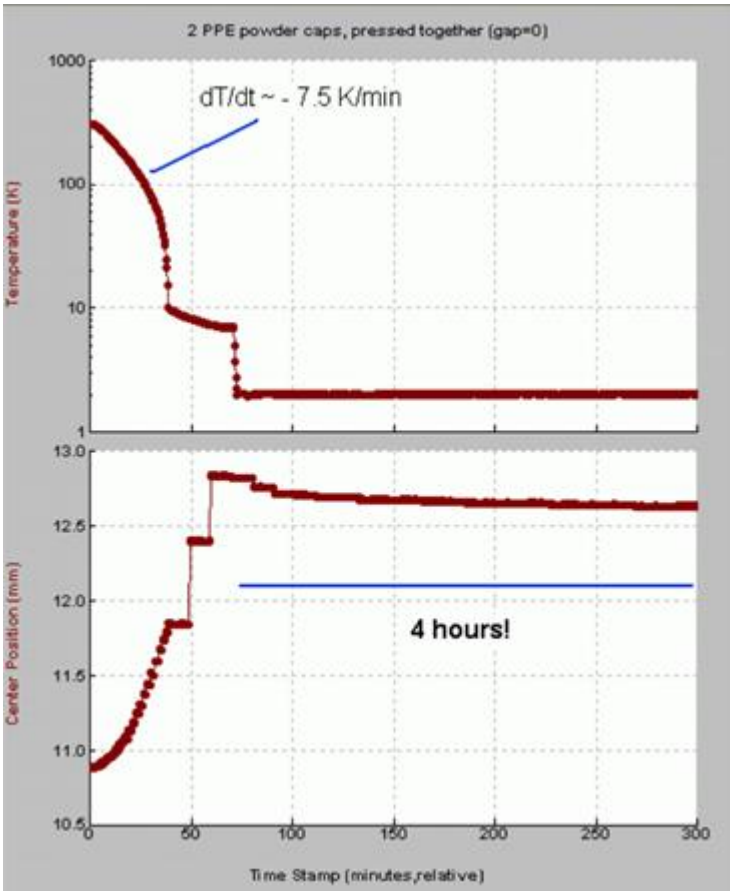

Figure 5.13: VSM data file for a moment vs. temperature sweep [37].

The reason that sample centering is so important is that the reported magnetic moment depends on the vertical position of the sample relative the center of the coils.

To understand how an error in vertical centering translates into an error in the reported moment, a centering scan on the sample must be performed.

Figure 5.14 shows centering scans for the sample measured here (left) as well as an ideal sample (right). The vertical axis corresponds to the magnetic moment in units of emu while the horizontal axis position is the motor position in units of mm. The sample used for this investigation was two empty VSM powder sample holders pressed together, and was chosen because the reported moment was a strong function of position. When measuring small magnetic moments, this often occurs because the magnetic "end effect" of the sample holder or other nearby material (like the powder capsules).

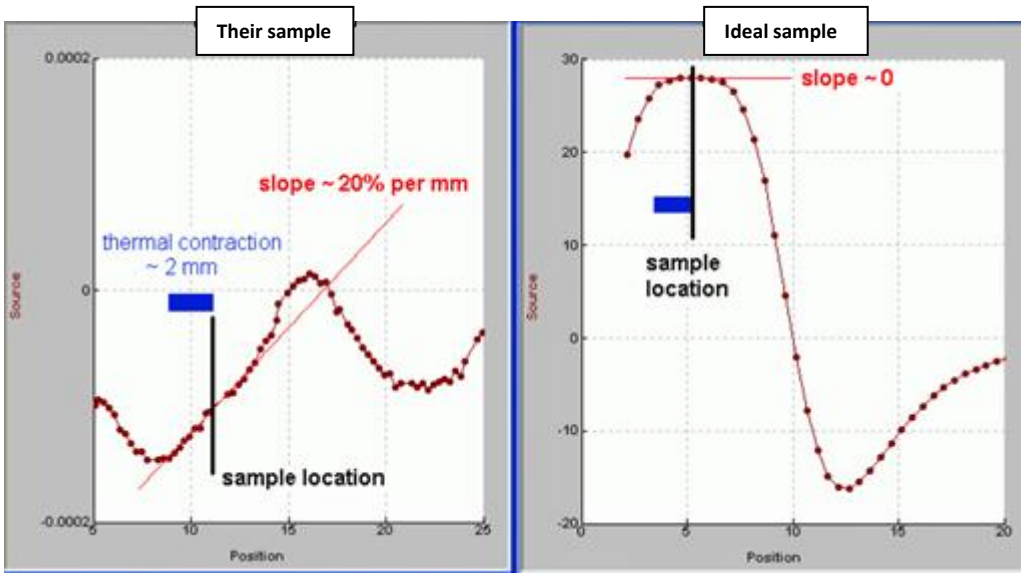

Figure 5.14: Centering scan error [37].

The linear motor in the VSM head uses permanent magnets. These magnets subject samples to approximately 200 Oe stray magnetic fields while they are being inserted into the instrument. These stray magnetic fields can cause some magnetic noise on the sample and measurements by pre-magnetisation of the sample.

For the Quantum Design driving system, the graph below shows the error in the reported measurement of a palladium reference sample as a function of axial position offset for a 2mm vibration amplitude.

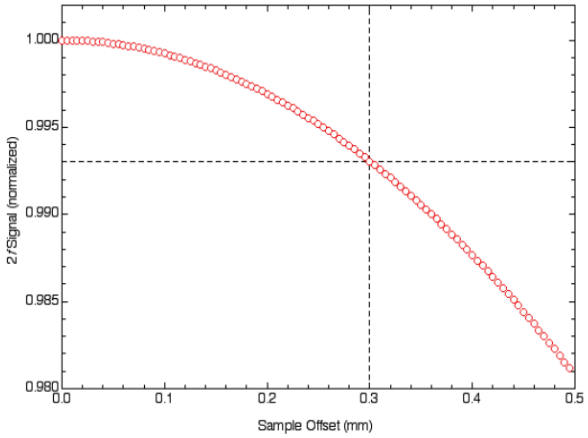

Figure 5.15: Sample offset accuracy [37].

When the sample has large magnetic signal ($>1 \times 10^{-4}$ emu) and produces a clean, symmetric signal for analysis, the sample position determined by the scan is typically precise to 10 μm. When the sample signal is weaker or the scan produces an asymmetric signal, the sample position determined by the scan may be precise to 50 μm. For very weak signals, large sample holder effects, and cases with magnetic contamination, the scan may actually produce meaningless data [39].

CHAPTER 6

DETAILED DESCRIPTION OF OUR SAMPLE DRIVE DESIGN

6.1. ELECTROMAGNETIC AND THERMAL ANALYSIS

The motor geometry designed emerges from electromagnetic analyses results. In order to acquire optimum gain from the motor, a series of analyses were executed. Unlike conventional round like linear motors, sided like magnet-coil binary was designed because accurate radially magnetized NdFeB magnets are unavailable in local markets.

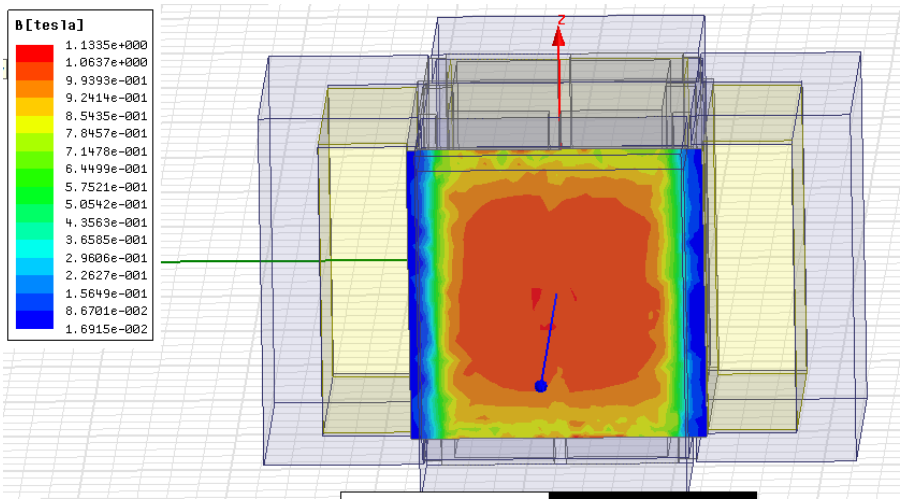

Figure 6.1: One-piece magnet design.

Unfortunately, another limitation was to find convenient size of the magnet on the market and the high expense of finding a one-piece magnet (Figure 6.1). Although one-piece magnets design have a strong magnetic field in the center, this maximum

field can not spread away from the center. Finally, 50x10x5 mm size magnets that are readily available on market were combined to obtain a one-piece magnet. Coherent electromagnetic analyses results proved that a number of magnets touching each other can act as a one-piece magnet because the iron yoke can hold the magnetic field stray in homogeneous distribution and in one direction due to fact that magnetic field strength is the same in unit volume of the magnets.

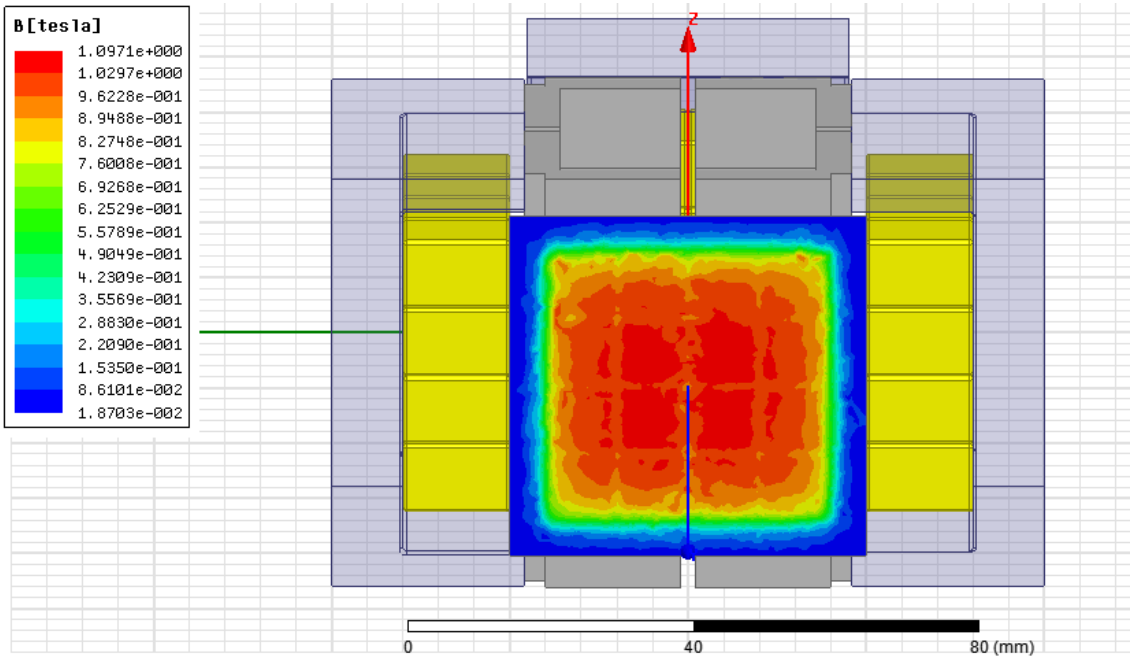

Figure 6.2: Conventional linear motor design.

In this design (Figure 6.2), it is striking that even though there are gaps between vertical magnets mounted together, lower values of average magnetic field distribution exist throughout the surface of the motor coil as localized point. This leads to an error named cogging in vertical direction. Cogging in conventional linear motors is one of the most common problems. To overcome this error, long rod magnets should be used along the motion of the motor coil.

Then, the hexagonal structure was designed. It is seen that 0.21-0.58 Tesla magnetic field acted on the motor coil but it was not adequate to accomplish the

mission. Since there are more turning points on the motor coil, force losses much as well as the interaction of each yoke block were very high in the hexagonal design. Thus, less magnetic field strength occurred in contrast to the expectations.

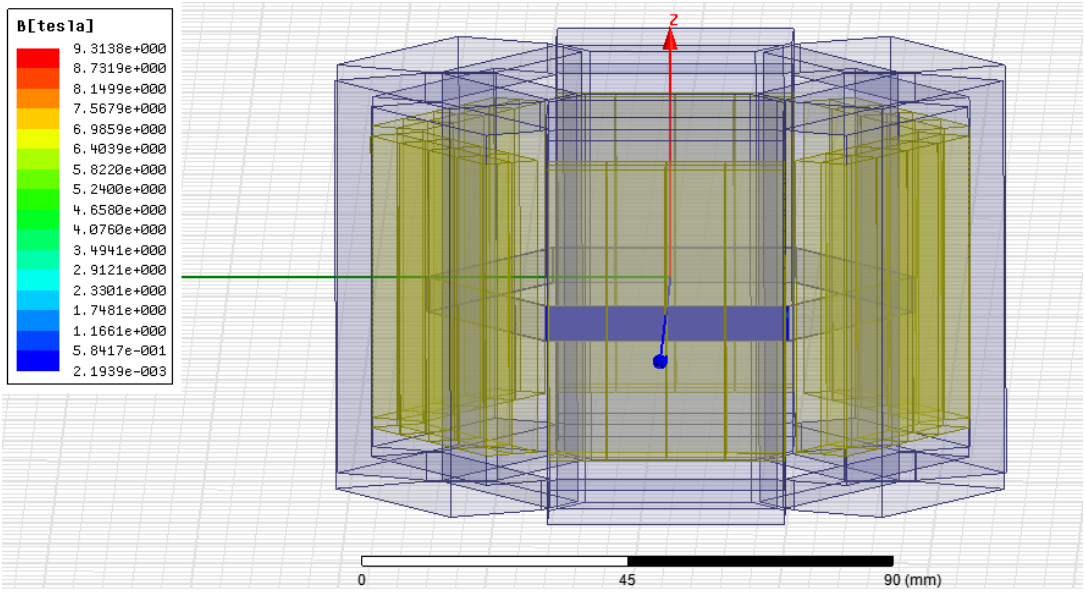

Figure 6.3: Hexagonal structure.

It was also challenging to mount the structure properly. Alterations in the design were unavoidable due to the fact that all attempts regarding the hexagonal structure have resulted in failure. Therefore, four magnet blocks that have a 90^0 angle between each other were implemented (Figure 6.4).

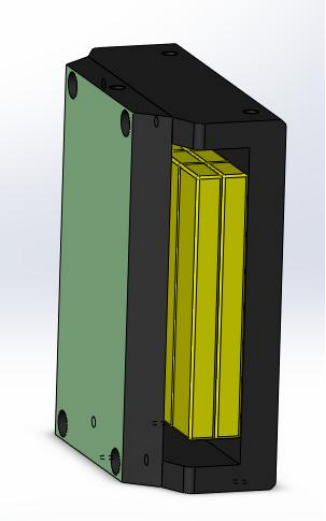

Figure 6.4: One of the four part of magnet block.

Next, attempts to design the optimum motor magnet geometry can be described as follows:

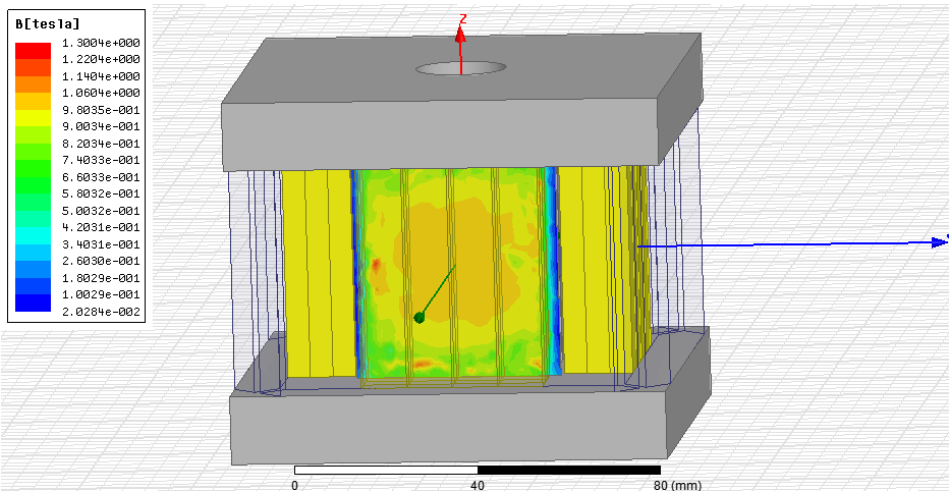

Figure 6.5: Fully-closed magnet & coil design

Fully-closed yoke design was performed but it was seen that the magnetic field distribution on the motor coil plane was very low and had some distribution deficits (Figure 6.5). It was also seen that the design with three magnets placed back to back was not a must because reduction from three to two magnets did not affect any of the values dramatically. Two advantage of using two magnets are that less cost and weight of the motor could be achieved (Figure 6.7). However, using a setting with one magnet unexpectedly reduced the magnetic field strength. It must be iron yoke for each face of motor coil. Therefore, four particular yoke parts were created and mounted using aluminum sheets. In this way, each part of the iron yoke did not only create its homogeneous magnetic field but also did not take in noise from the environment and show a chaotic distribution. In fact, any machining performed on the yoke lead to disturbing values of the magnetic field. There must be very few indentations and edges where the magnetic field will turn and they must be as smooth as possible.

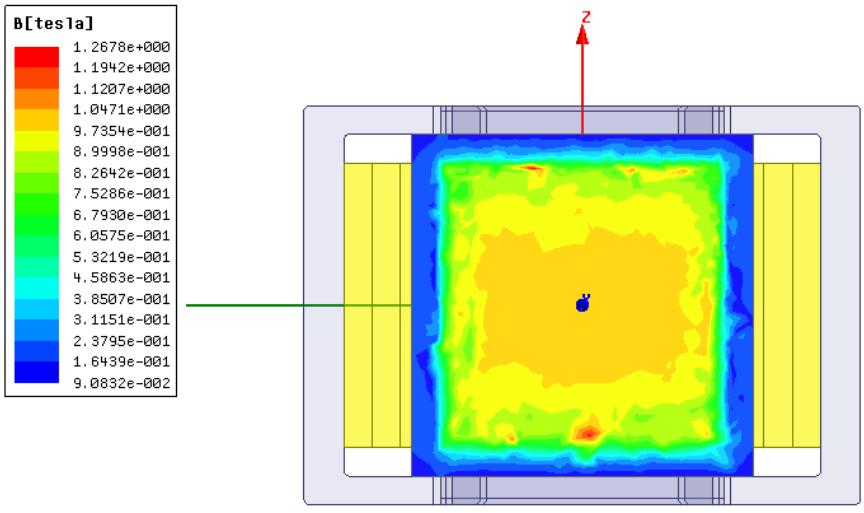

Figure 6.6: 3-set magnet design.

Actually, one disadvantage of the 3-magnet design is the gap between the yoke and the coil surface that reduces the magnetic strength distribution chaotically and gathers the maximum values of the magnetic field just in the vicinity of the center point as seen in Figure 6.6

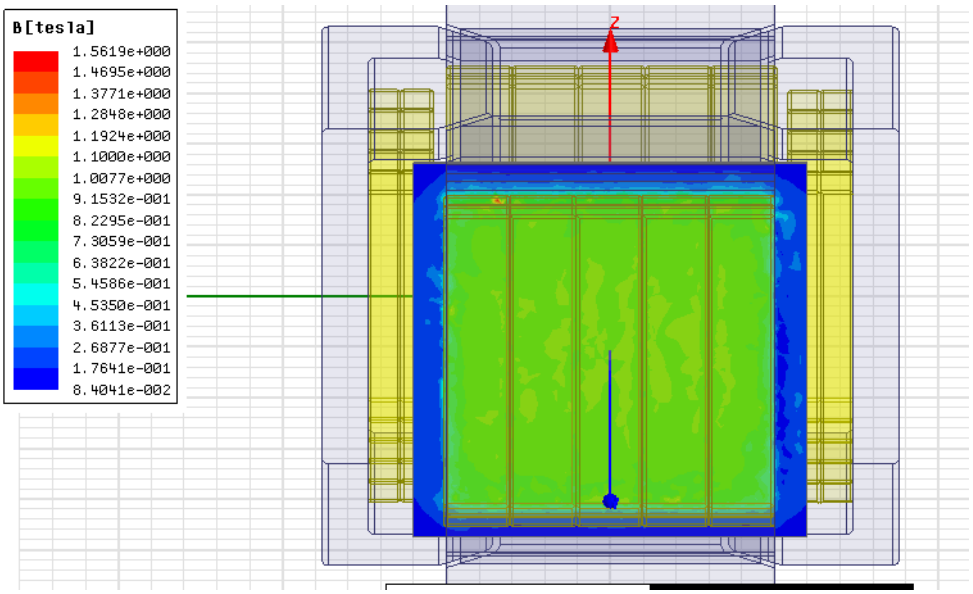

Figure 6.7: 2-set magnet design with thick iron yoke of 10mm.

Although, the maximum magnetic strength was enough to achieve the desirable motion capabilities, distribution of the magnetic field on the stroke distance was not homogeneous. Increasing the thickness of iron yokes also leads to a reduction in magnetic field strength (Figure 6.7). That's why, thickness of the iron yoke had to be reduced by a few milimeter.

Finally, in this design, the thickness of the iron yoke changed to an optimum value of 5mm (Figure 6.8).

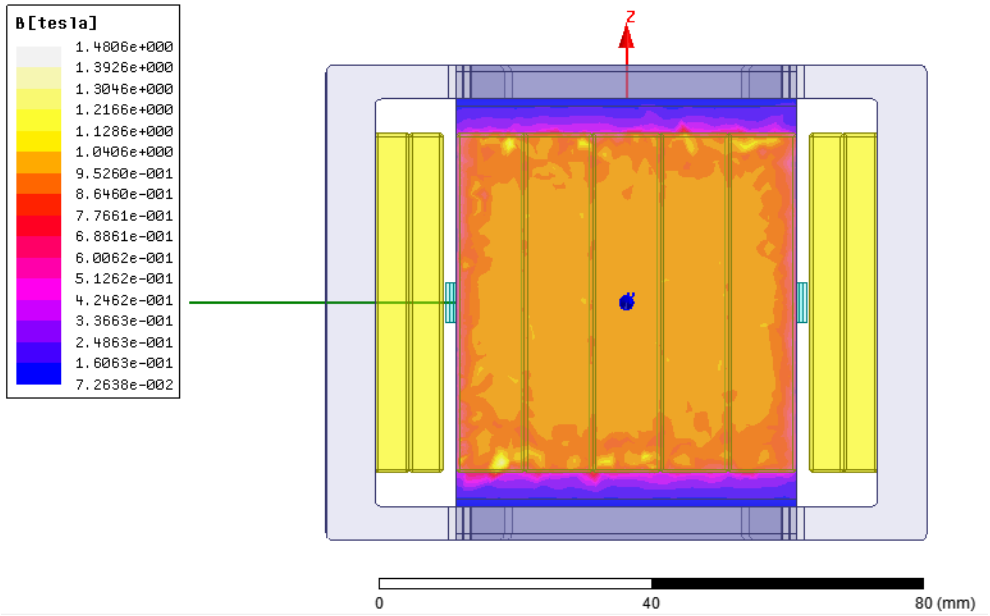

Figure 6.8: Magnetic flux density on motor coil way.

The stroke value of the motor is 60 mm, but the magnetic distribution along that distance is not constant, that is, the Lorentz Force that affects on the motor coil will not be the same throughout the stroke distance. Based on the design, the maximum field distribution is necessary at ± 20 mm from middle point of stroke, spanning 40 mm in total. As a matter of fact, the maximum frequency and amplitude of the desired motion are not necessarily between the higher and lower limits of the stroke. There must be a distribution having the maximum average in the active zone. In previous designs, we observed low values of distribution of magnetic strength in local points on the motor coil surface. Hence, it means that the motion will not be accurate throughout the stroke range, in other words, the active force on the motor coil will not be able to sustain constant speeds. If such localized areas exist, no matter how effectively you use feedback, there will be some noise in the VSM measurement (hysteresis loop). Thus, desired values of sensitivity cannot be reached. Finally, one important point to note is that the more magnet surfaces are close to the coil surface, the more magnetic field strength is forceful. Provided that the mounting can be done easly and no severe rubbing or friction exist between the parts, the distance between the magnets and coil surface can be reduced to 0.4-0.5 mm. The fact underlying this situation, is that the magnetic stray fields will bend as the field goes further from the

magnet. So, if the distance is short enough, these stray fields arrive at the coil surface perpendicularly.

This Maxwell analysis illustration exhibits approximately 0.95-1.0 Tesla magnetic field on the coil wire (Figure 6.8).

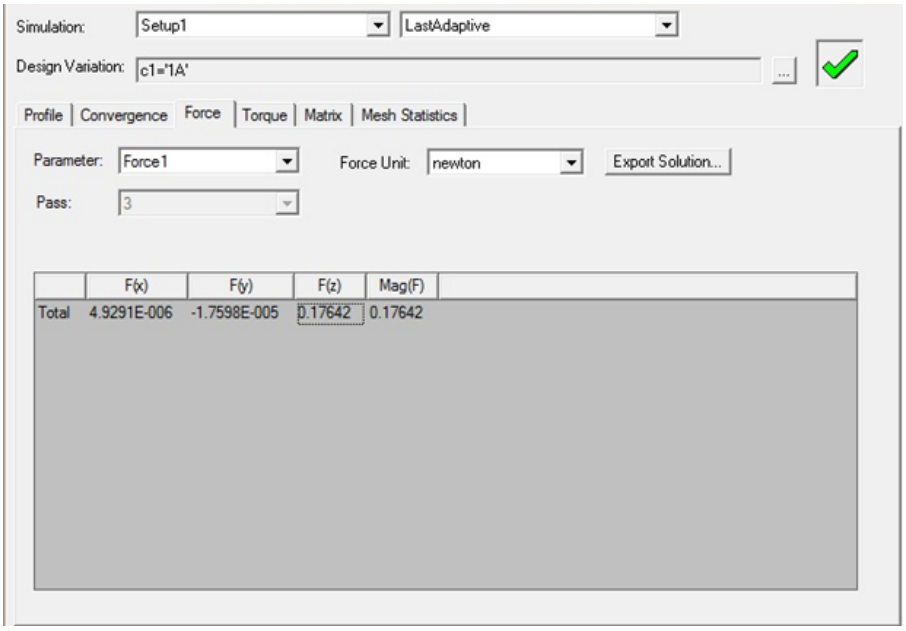

Figure 6.9**:** Calculated force on the motor coil in Z direction for only one turn.

Force value along the z direction is about 0.176 N per A for a single turn. Multipliying this value with number of turns, 8.44 N per A will be obtained for 38 turns. Note that the total weight of all moving parts is almost 150 gr, hence, it is possible to obtain 56 m/s^2 acceleration per 1A.

Table 6.1: Theoretical expectations from motor motion.

Current (A)	Freq(Hz)	Amp(mm)
5.4	10	21.3
5.4	20	16.3
5.4	30	12
5.4	40	6.3
5.4	50	4.9
5.4	70	2.5
5.4	80	2
5.4	100	1.2

Some parts of the motor that are vulnerable to temperature originating from the current applied to the motor coil are analysed and thermal expansion effect is investigated by Solidworks temperature simulator. Based on the thermal expansion of the parts, we designed all components with an effective tolerance. Otherwise, termal effect may cause more friction due to thermal expansion of the crucial components.

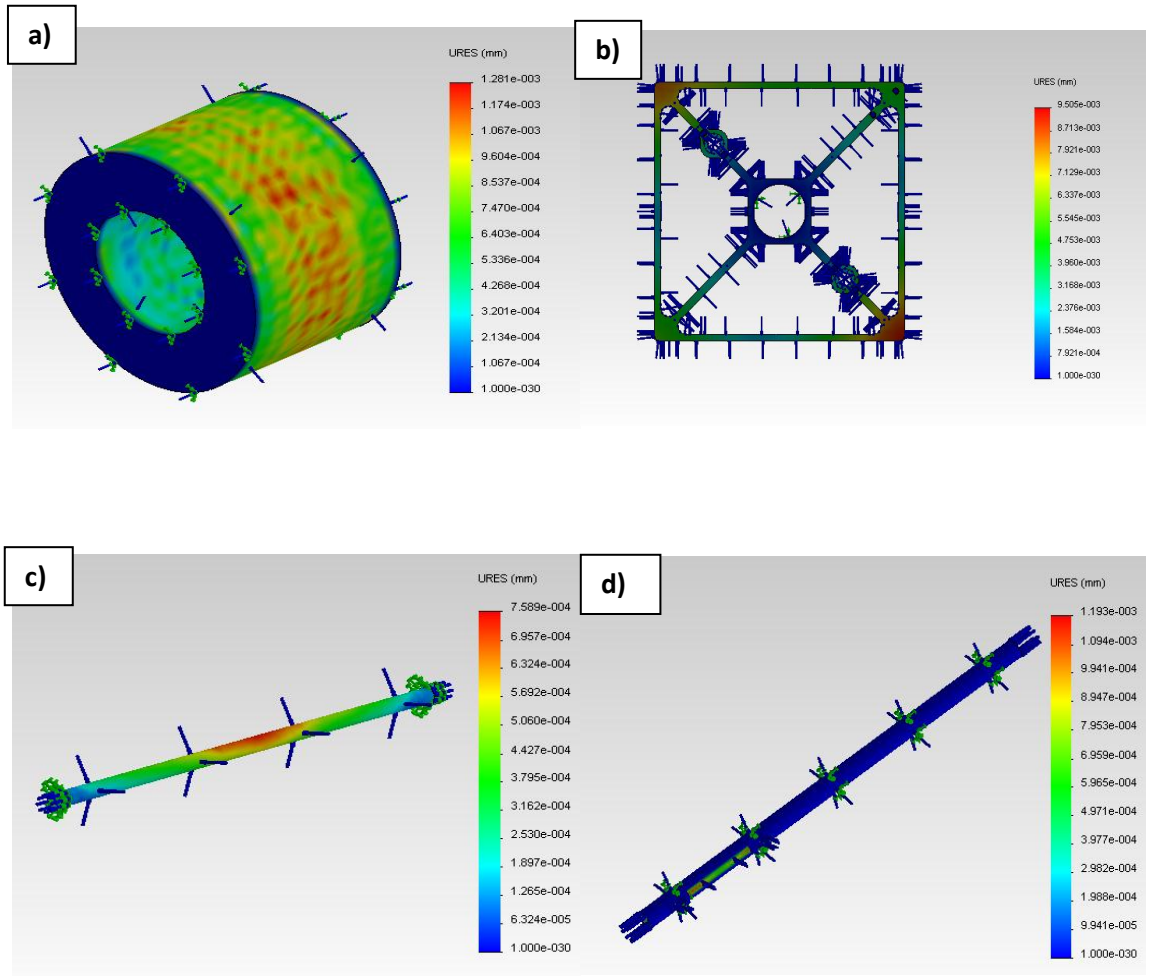

Figure 6.10: a) Rulon bearing b) Motor coil part made of aluminum c) Motor shaft made of aluminum d) Steel rod

6.2. MECHANICAL DESIGN

Sample vibrator is an important part of the VSM which is built to fulfill the principle requirements, namely, generating pure sinusoidal vibrations of constant frequency and stability of vibration amplitude of the signal [40].

Although most of the VSM systems have good control devices that successfully fulfill the tasks successfully, the most important challenge is to design

and manufacture a convenient linear motor to obtain sinusoidal motion with constant frequency and amplitude. Besides that, frequency and amplitude must be changeable to higher or lower values depending on the conditions of measurements so as to enhance sensitivity of VSM measurements.

In the light of previous studies throughout the history of VSM, we decided to design a unique linear motor depending on Lorents Force Law in order to move the sample linearly in terms of both electromagnetic and mechanical balance. We used conventional control devices with a unique linear motor which can respond to all motion requirements for control signals. In this design, we utilized some common software package for analysis that enable us to foresee the correct design before manufacturing. Also, in this system, all obstacles that disturb effective motion were solved mechanicaly in Figures 6.11 and 6.12.

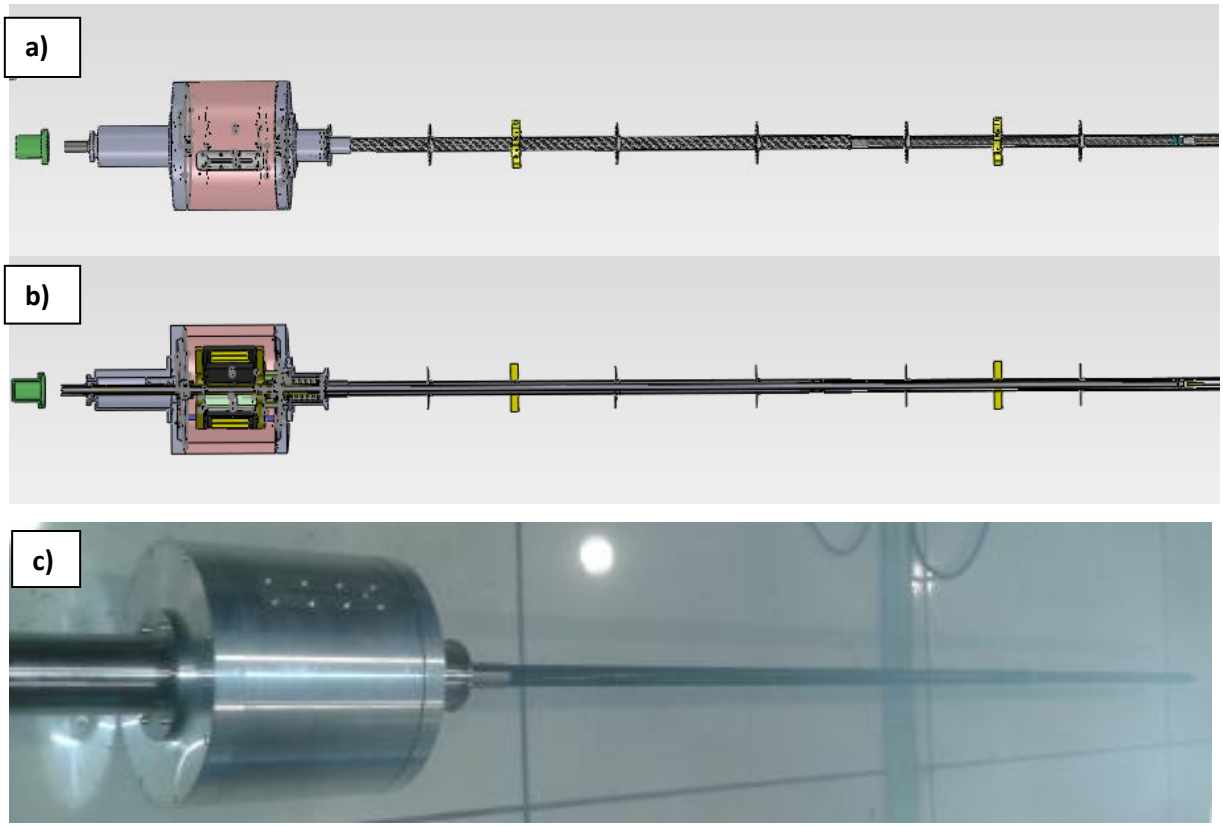

Figure 6.11 : a) General view of CAD drawing of VSM system, b) Cross-sectional view of VSM system, c) real image after producing with extension of the probe rod.

One of the most important features of this linear motor is to have free stroke motion ability which a classical loudspeaker does not have. That enables us to control the sample position and locate the sample in the middle point of pick-up coils automatically. Advanced optic encoder is the most critical component in this process because it plays a key role in the accuracy of measurements.

The covering frame of the motor is made of aluminum in order to reduce the total weight of the system and is surrounding the motor and preserving the vacuum. Although aluminium is highly vulnerable to abrasion, it is better to use aluminum because it stays stationary. To preserve the vacuum, two stainless steel flanges were screwed to the upper and bottom ends of the cover. In addition, top flange also provides us with a slot to fix the encoder and bottom flange provides us with the slots to both embed the helix spring and fix the carbon fiber tube. In order for the user to hold the sample rod easily, a delrin aparatus was attached to the edge of the sample rod (Figure 6.20). Also, this delrin component keeps the rod away from cracking. Two ring magnets were employed to catch these sample rod and moving aluminum shaft that is mounted to the motor coil bobbin in Figure 6.12. In order to preserve the vacuum, a stainles steel dome with an o-ring was placed onto the whole system by a sealing o-ring.

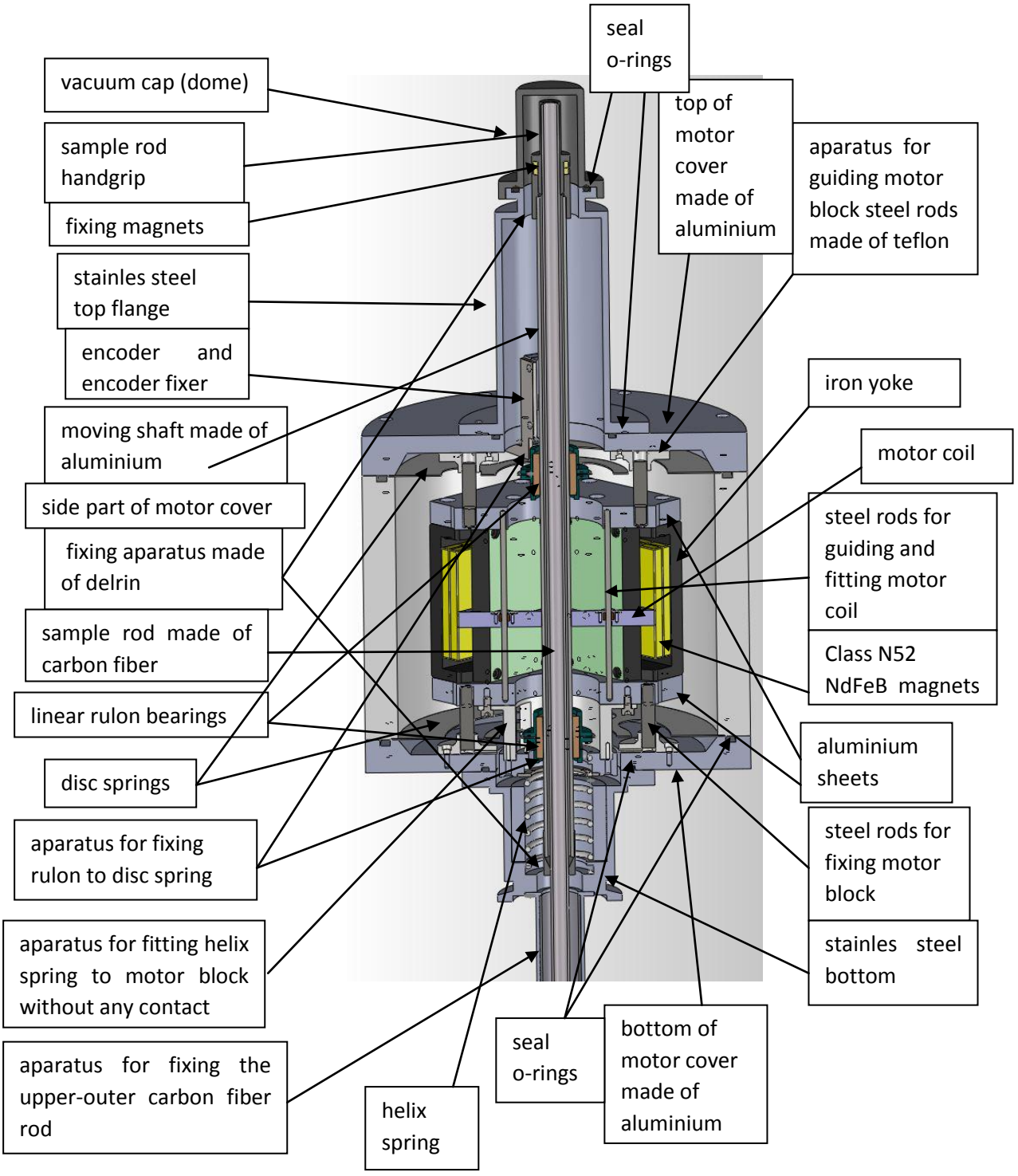

Figure 6.12: Detailed description of the linear motor design in cross-section view.

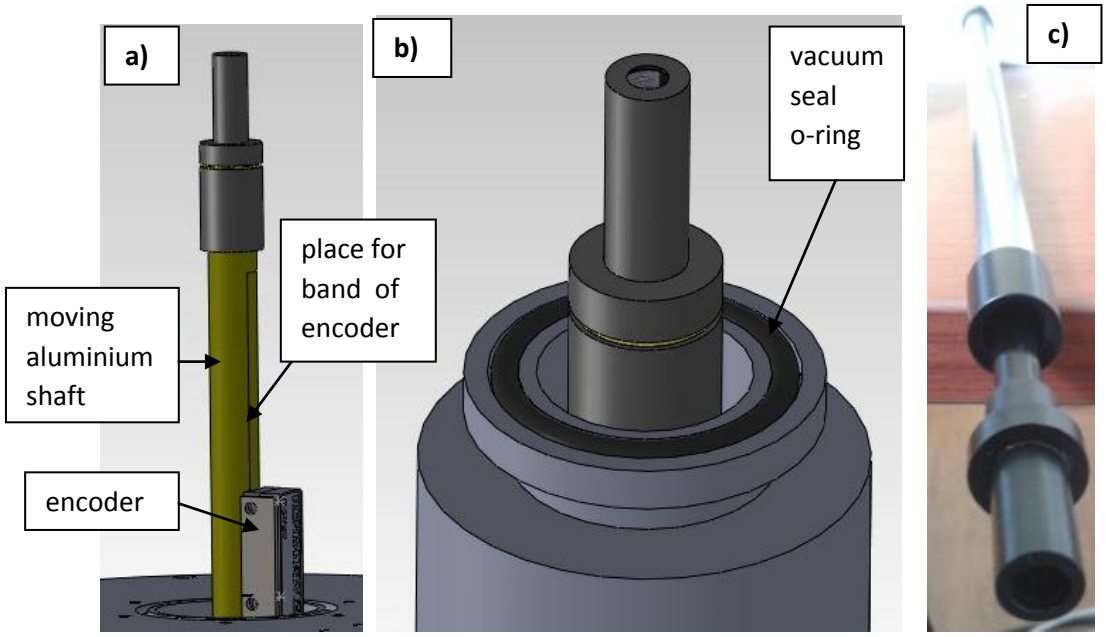

Figure 6.13 : a) encoder and place of the band on the shaft. b) Entrance of the sample rod and enclosing the section of vacuum with sealing o-ring. c) Sample rod is being fixed to motion provider aluminium rod through two magnets. Vacuum seal o-ring (in the middle) was used as a vacuum cap in Figure 6.14.

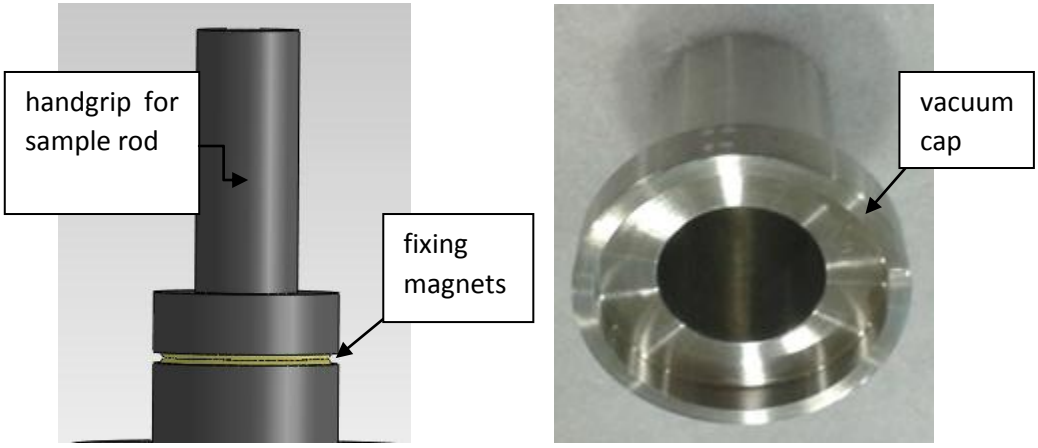

Figure 6.14: Fixing magnets(on the left) and stainless steel vacuum cap (on the right).

Fixing magnets are very useful in attaching the sample rod to the moving shaft. 15x11.4x3 mm size of two N35 type ring magnets were used. Vacuum dome

made of stainles steel in Figure 6.14 was used to seal the vacuum without any locking mechanism.

On and under the motor block, aluminum sheets were used for both keeping the four separated yoke blocks together and for holding the whole yoke block concentric. Moreover, four stainless steel rods threaded at one end were attached to these aluminium sheets in order to prevent rotation of the yoke blocks in Figure 6.15. Four teflon components were mounted to the top and bottom covers so that the four rods can slide smoothly.

Unique rulon sleeve bearings are very useful in sustaining the concentric motion by guiding the moving shaft. Rulon bearings only guide the aluminium shaft by means of mounting it to disc springs as shown in Figure 6.15(c). Rulon bearings were preferred because they have much lower friction and thermal expansion coefficients than teflon. Disc springs were designed with patterns in them and are only helpful to fix the rulon bearings through some auxiliary components. These patterns were turned into grooves by laser cutting process (Figure 6.15(b)). These disc springs are, in fact, most vital components that help holding the rulon bearings in concentric axes and in linear direction during sliding without any mechanical vibration or contact. If these discs were produced or designed wrongly, the motion in concentric axes would not be achieved properly.

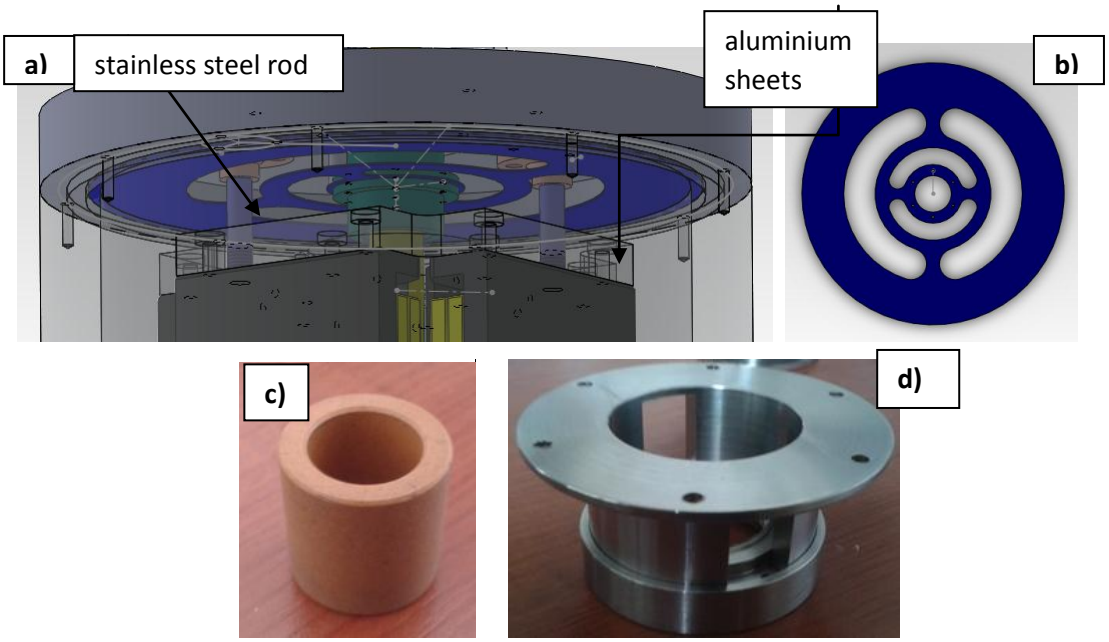

Figure 6.15: a) Steel rods and aluminium sheets cover the motor blocks. b) Custom design disc springs. c) Rulon Bearing d) Aparatus to combine yoke block to helix spring

In order to combine the yoke block to the helix spring without any contact with the disc spring, an important component was employed. This component was adjusted in accordance with the grooves of the bottom disc spring and allows for mounting the yoke block to the helix spring without any contact with other components (Figure 6.15(d)).

Helix spring enables the yoke block to make smooth vibrations up and down. This vibration is approximately 1-3 mm in amplitude according to the frequency of motion and is caused by the reaction of the force induced on the bobbin by the magnets (Figure 6.19a and b).

Nearly pure iron ST-37 was used as yoke material because of its low C concentration. This yoke consists of four concentric circles contained in each another (Figure 6.12). These four parts were combined by aluminium sheets mentioned above. Class N52 NdFeB strong magnets were mounted to each four components of

the yoke block as shown in Figure 6.16. Bobbin of copper coil was made four-sided because accurately arranged radial magnets are not available in the market. To benefit from each unit lenght of the coil and magnets, a significant portion of their areas were brought face to face. By this way, more force could be induced on the coil by the fixed magnets as in Figure 6.16.

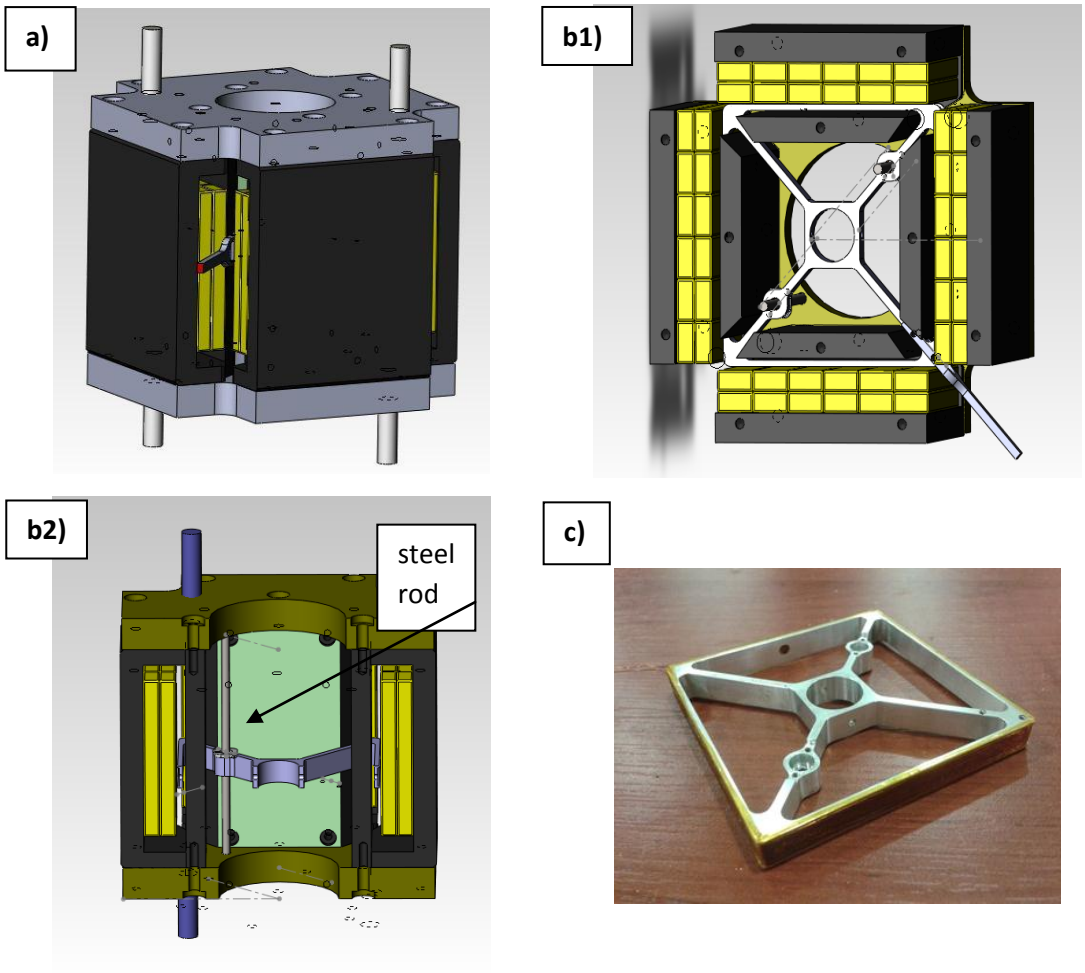

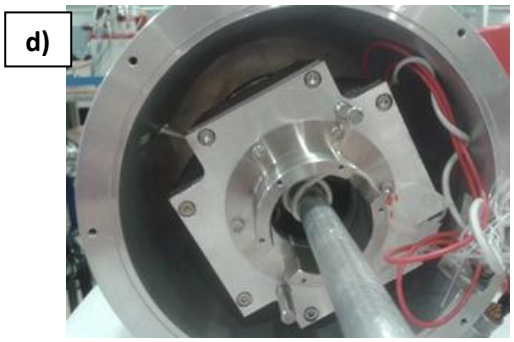

Figure 6.16: a) general view of motor mechanism from bottom, b1,b2) cross-section view of motor mechanism, and c) motor coil d) motor and moving shaft with their data cables.

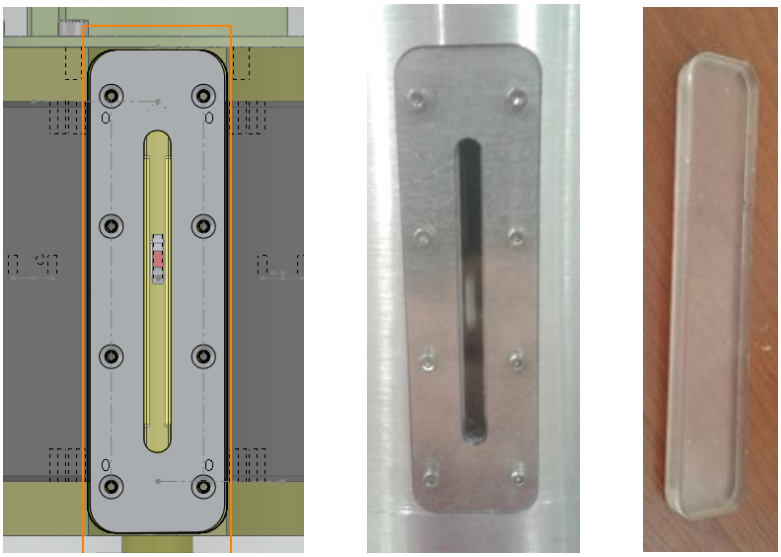

Figure 6.17: a) CAD skecth of indicator screen. b) real image after producing c) plexy glass.

Indicator screen helps us know where the sample is and this indicator point (red one) is visible through plexy glass of 5 mm thickness (Figure 6.17).

Helix spring as the main spring has 2.5mm diameter of wire, 30 mm outer diameter, 65mm free lenght, and 8 active coils and is made of stainles steel A304. In the light of these quantities, the helix spring has 2030N/m spring constant, a

resonance frequency of 32 Hz and 50mm loaded length at 3 kg yoke block weight. Furthermore, at trailing outer diameter of the spring, there is a teflon tube to keep spring vibrating without any wriggle and with less friction in Figure 6.19.

Not only a linear motor that can move at a perfect sinusoid has to be designed and manufactured, but also the mechanical noises, that are likely to disrupt the motion from being sinusoidal, must be avoided. For this purpose, carbon fiber tubes that have a highly stable rigidity in any condition and protects its high strenght in a wide temperature range. They also ensure unbending of the structure up to a critical length. Both the sample rod and its guidance are selected from the same material because the guidance carbon fiber tube which will carry the detection coil assembly and sample on the sample rod must be in the same line horizontally. So, any thermal agitation affects each two in the same way and therefore their sizes will change equally.

When the user places the sample rod into the probe: First, fixing magnets hold the sample rod from its top as a first holding point. Second, as the sample rod passes through the teflon bearing in the middle of the guidance carbon fiber tube, the sample rod will slide through the linear bearing as a second holding point. As a result of fixing at the two points, sample is now ready to move together with the aluminum shaft (Figure 6.13(c)).

Radiation shields and the apparatus that enable us to fix the carbon tube to G-10 tube in the cryostat are shown in Figure 6.20.

A lemo connector was used in order to take out the cables coming from the encoder and moving coil without any vacuum leakage Figure 6.18. Additionally, a monitor for indicator pin was attached to the front of the outside cover through a slot in order to monitor the motion of the coil and estimated position of the sample shown in Figure 6.17.

In this motor mechanism, we used ST-37 material as yoke metal because of very low carbon concentration (0.01 %) and N52 class strong neodmium magnets (yellow) and this combination produced approximately 8.13 N/A Lorentz force,

linearly. Besides that, in order to fix the yoke blocks, we used aluminum plates on the top and bottom. In Figure 6.16(c), an aluminum bobbin pulley is used for possible torsion or flection during the motion. So as to hold the coil pulley in one direction without rotating, we utilized thin steel rods-teflon bearing couple as in Figure 6.16(b1). As motor coil wire, we used pure copper with 0.28 mm in diameter and about 9.12 m in length. This size permits us to transmit 7-8 A current without any heating problem.

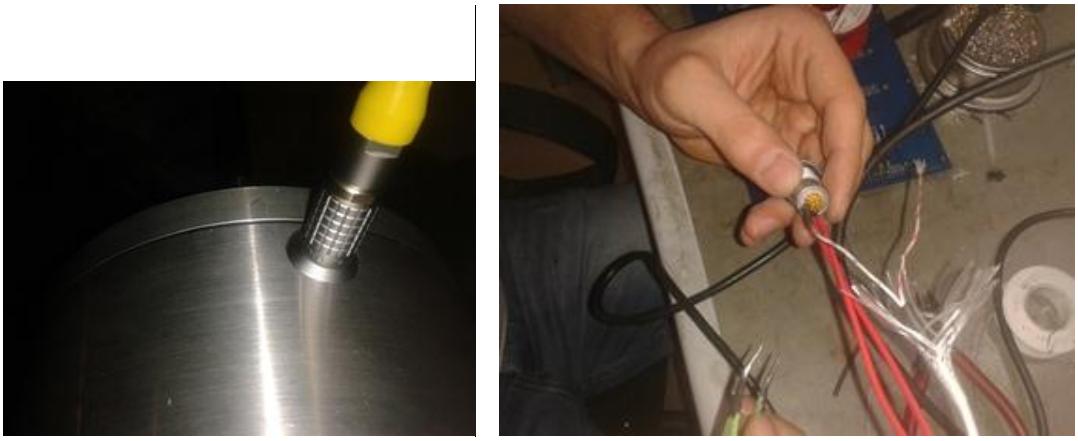

Figure 6.18: Lemo connector.

Data cables from encoder, bobbin and thermocouple are taken out from vacuum conditions to atmospheric conditions through a Lemo connector securely (Figure 6.18).

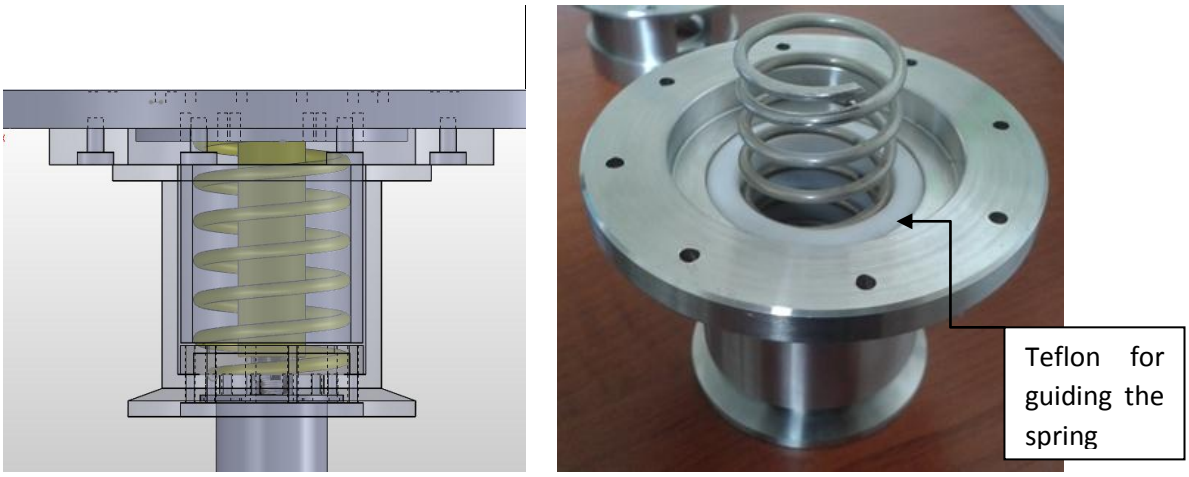

Figure 6.19: Main helix spring that supports the weight of the motor block is positioned under the motor block.

The stainless steel spring has a spring constant of 2030N/m and supports the yoke's weight in one direction. Real image of the helix spring and the flange that holds the helix spring are given (on the right hand side in Figure 6.19). The spring was used as a damper to reduce the vibration of the motor block, which means that the motor has a self-contained mechanism to damp the vibrations. A teflon tube was employed for guiding the spring smoothly.

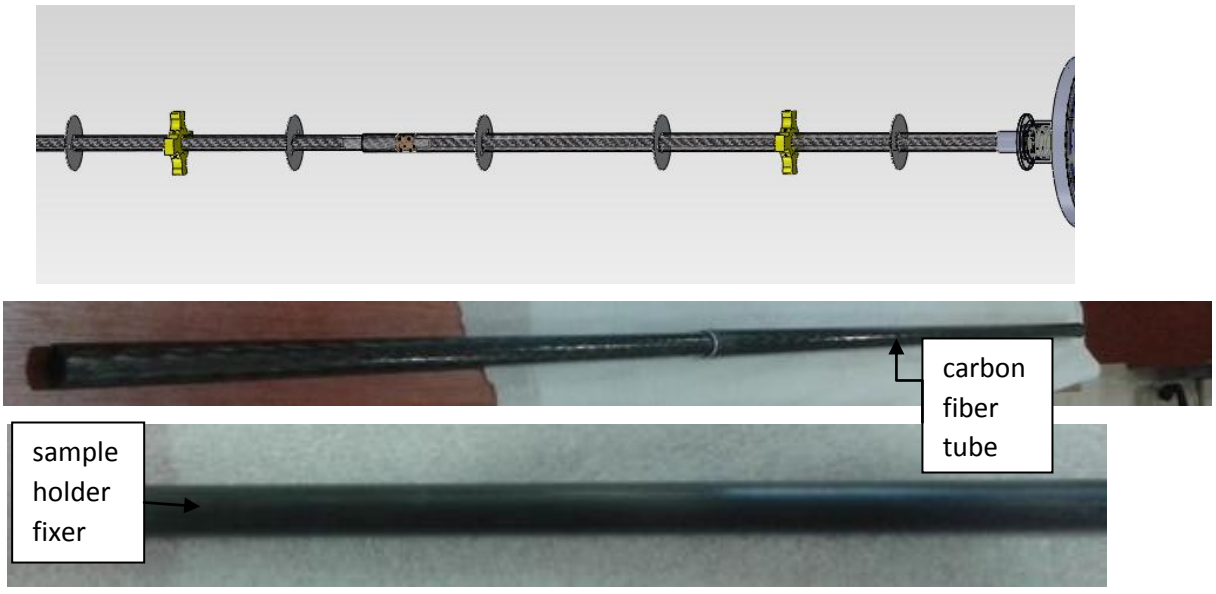

Figure 6.20: Carbon fiber tube combination.

Carbon fiber tube combination provides us with the ease of probing the sample by means of stiffness and unflexibility properties, and that of pick-up coil mechanism into the cryostat that has superconducting magnet up to 10 Tesla and cryogenic temperatures up to 1,5 K^0. In the medial image, it also carries some radiation shields and fixing parts (yellow ones) that enable us to fix the carbon fiber tube to G10 tube in the cryostat gap. Moreover, carbon fiber rods can resist low temperatures. A fixer for sample holder was produced from delrin shown in the bottom image (Figure 6.20). Most importantly, carbon fiber and other materials close to the measurement site are non-magnetic, thus any magnetic contribution on the sample will not ocur.

Figure 6.21: Sample rod guiding and extension mounting.

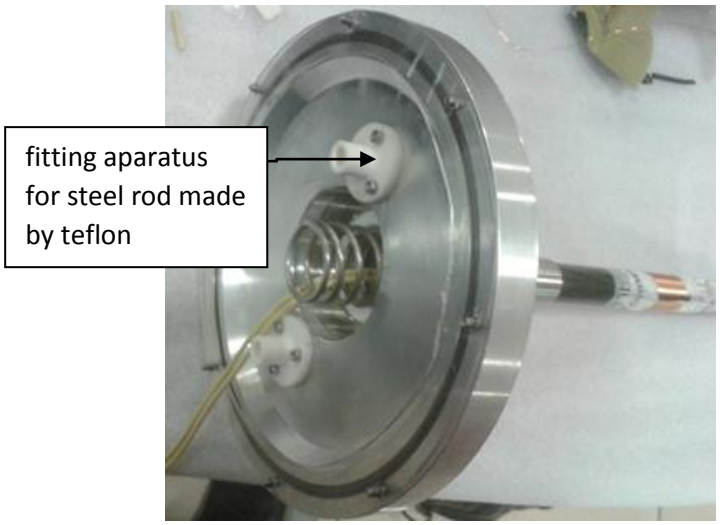

Figure 6.22: Bottom motor cover and parts on it.

On the right, there is an extension apparatus made of aluminum to attach two carbon fiber rods together, and it contains a linear self-lubricated bearing (purple) to guide the carbon fiber extension of the moving shaft (Figure 6.21). A convenient teflon sliding aparatus was designed to hold the motor block steadily (Figure 6.22).

6.3. MANUFACTURING

To manufacture the components of the linear motor, three different CNC machines were used as illustrated in Figure 6.23. These machines are capable of processing all metalic and plastic materials that we used. Therefore, we can produce and mount all parts of the motor without any mechanical restrictions.

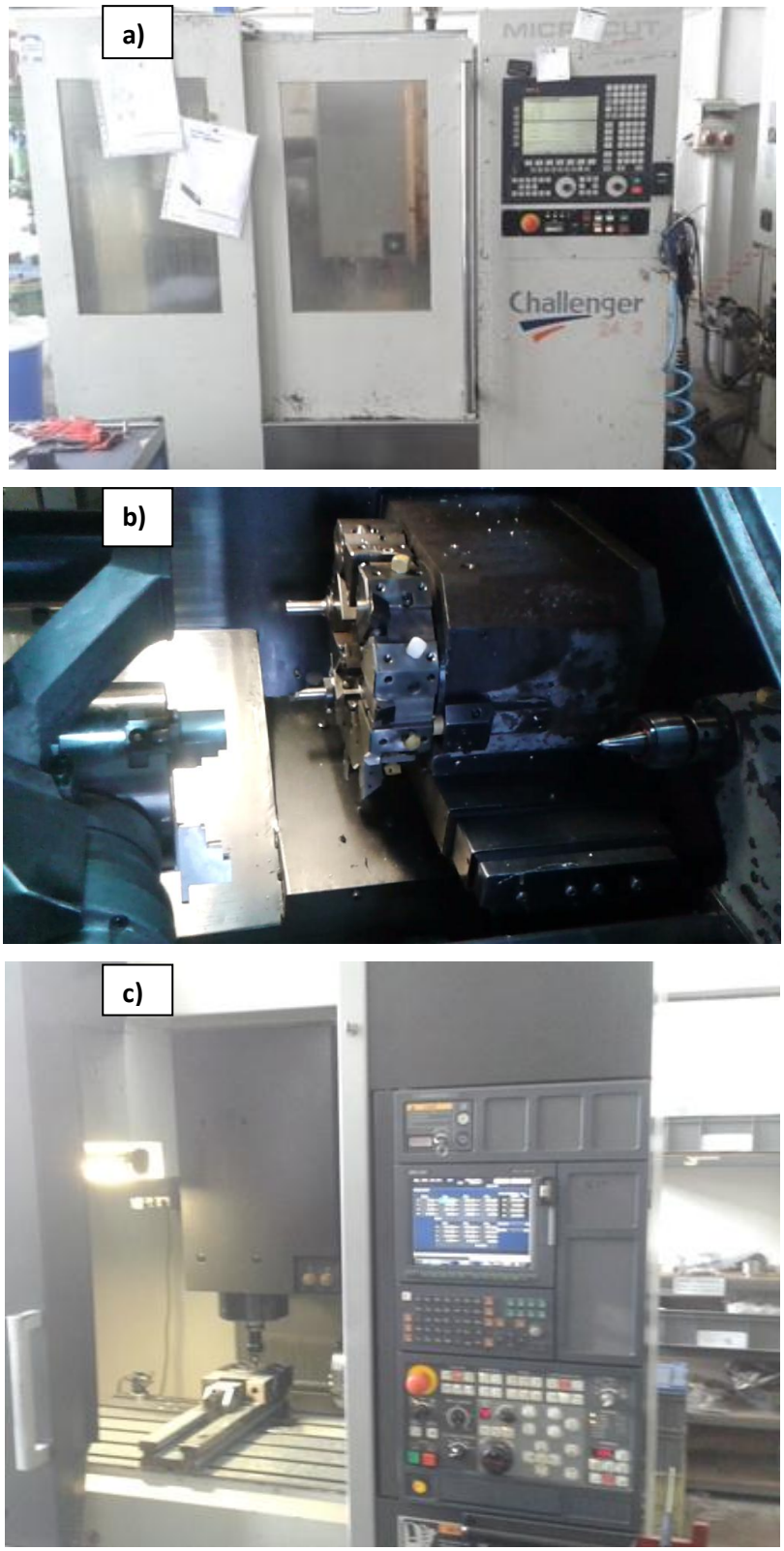

Figure 6.23: a) Microcut CNC fraise, 3-axis, b) Mazal turning machine, automatic c) Mori Seiki CNC fraise, 4-axis

CHAPTER 7

FEEDBACK FOR LINEAR MOTOR

7.1. ACCURATE MEASUREMENT OF LINEAR SINUSOIDAL MOTION

A linear encoder is a sensor, transducer or readhead paired with a scale that encodes position. The sensor reads the scale in order to convert the encoded position into an analog or digital signal, which can then be decoded into position by a digital readout (DRO) or motion controller.

The encoder can be either incremental or absolute. Motion can be determined by change in position over time. Linear encoder technologies include optical, magnetic, inductive, capacitive and eddy current.

Linear encoders can have analog or digital outputs. Analog output for linear encoders is sine and cosine quadrature signals.

Incremental encoders with built-in digital processing make it possible to transmit position to any subsequent electronics such as a position counter. As well as analog or digital incremental output signals, linear encoders can provide absolute reference or positioning signals[41].

In this study, RGH25F linear optical digital incremental encoder from Renishaw was used. It can operate in UHV conditions and reach 0.1 μm resolution at about 3 m/s speed; that means it permits 300 Hz/s at 5mm amplitude as shown in Figure 7.1.

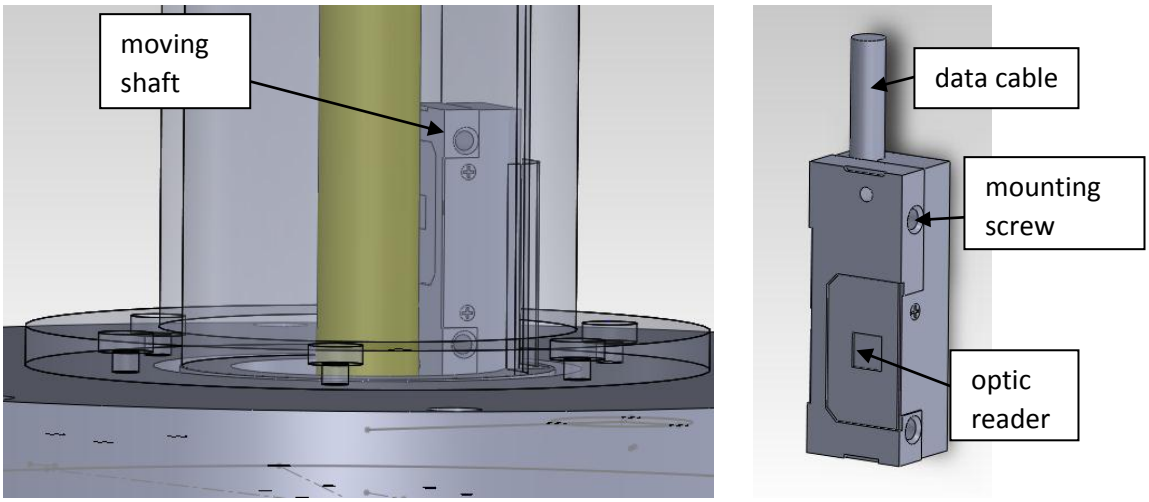

Figure 7.1 : This image illustrates mounting of linear optic encoder unit.

Encoder takes position information of the sample from the thin band attached on the moving shaft of the motor, and has at least 1 μm sensitivity.

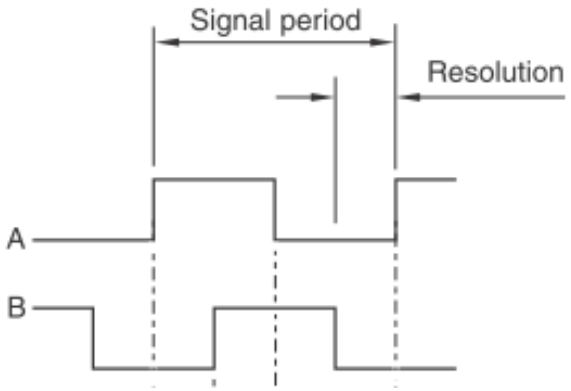

Figure 7.2: Digital output signal of the encoder.

Principle of operation of the encoder depends upon the counting method of the signal (Figure 7.2).

Encoder mounting and testing was not included in this study but the motion was tested by simple Faraday magnetic induction law instead, which will be explained in Chapter 8.

CHAPTER 8

TESTS AND RESULTS

8.1. TEST EQUIPMENTS

For conducting the motion tests, some driver circuits that enable us to make preliminary tests without any feedback were utilized. This motion here was the pure motion capacity of the linear motor and we observed how mechanical friction could prevent the motor from moving simultaneously with the signal coming from the signal generator. Moreover, we benefited from Faraday's Magnetic Induction Law claims that if a magnet moves inside a selonoid, a small AC voltage will be induced in the selenoid proportional to the frequency of motion of the motor. To achieve that, we attached a magnet on the moving shaft (Figure 8.2b) of the motor and put a coil on the outer carbon fiber tube in Figure 8.2a. Moving shaft moves the magnet so that the induced voltage in the coil appears on the oscilloscope after passing through a differantial amplifier, and finally we can see the signal properly.

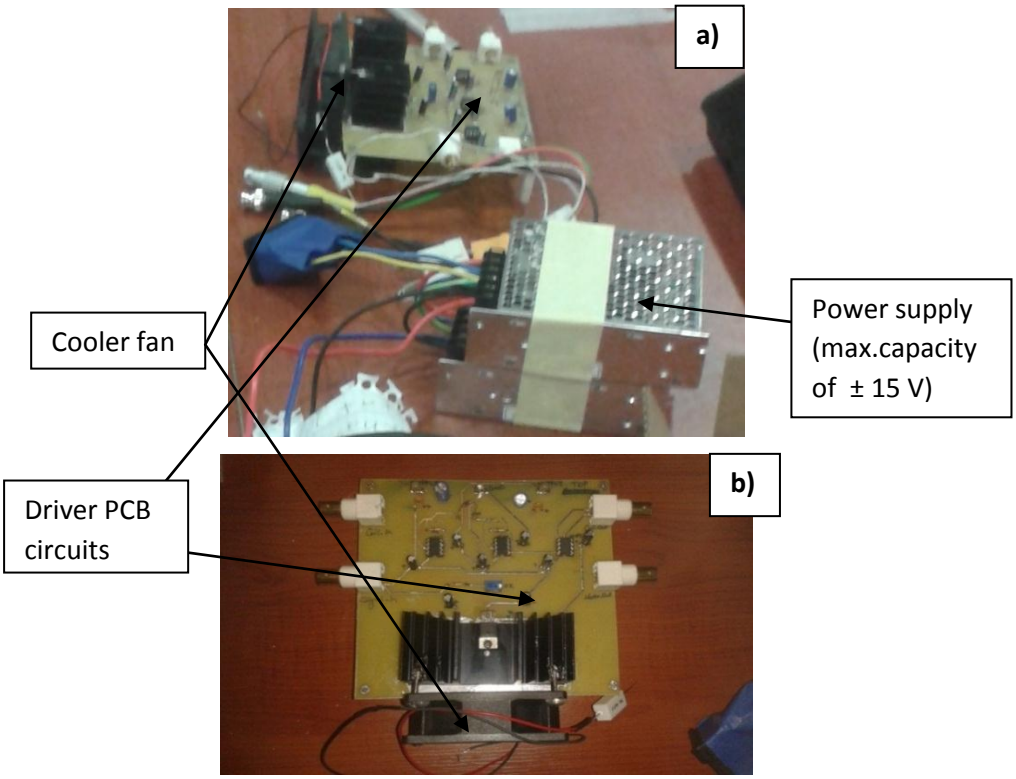

Figure 8.1: a) driver circuit contains driver PCB and power supply. b) detailed image of PCB.

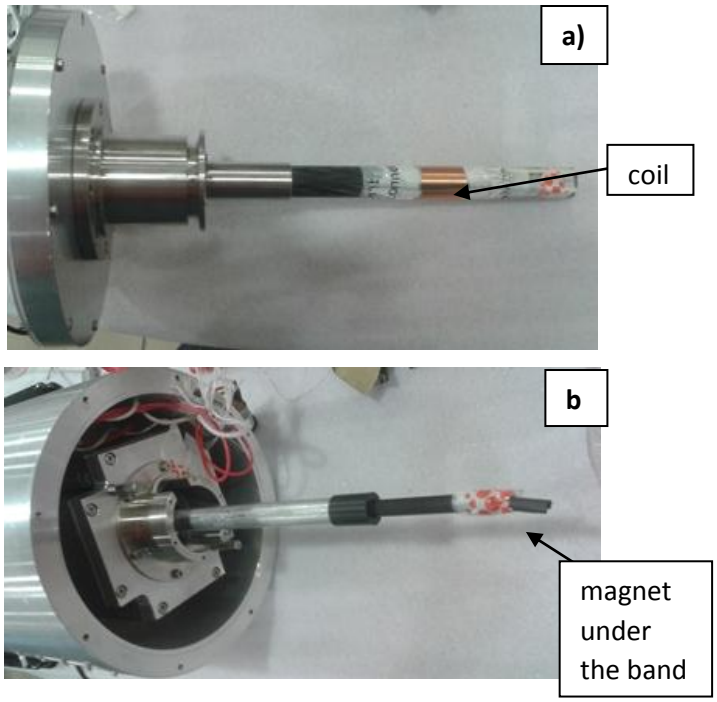

Figure 8.2: a) Coil for taking signal from motion b) magnet for inducing a voltage into the coil.

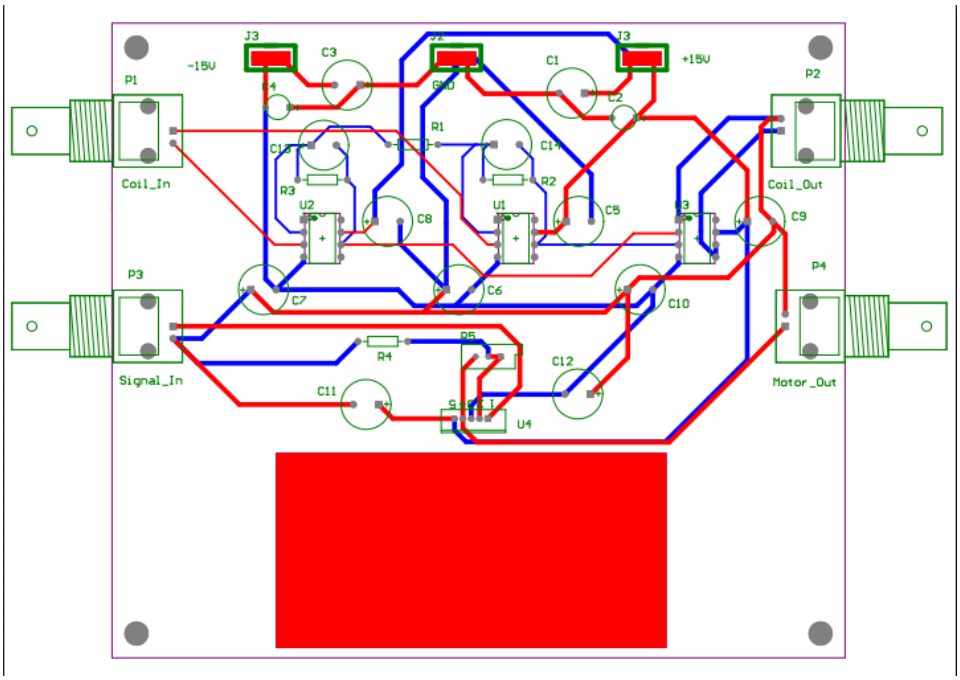

Figure 8.3 : Motor drive PCB circuit

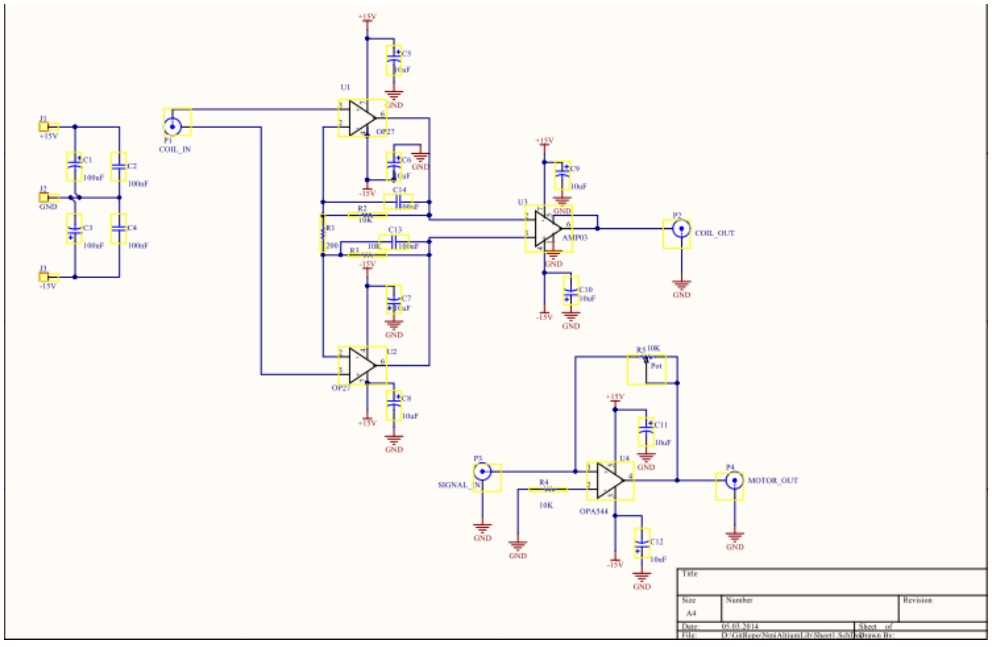

Figure 8.4 : Motor driver circuit schematic representation.

This motor driver PCB contains two circuits shown in Figure 8.3 and Figure 8.4: First (top) is the one whose input is the signal that comes from the coil to induce a small AC voltage to obtain the displacement of the motor, ((R2+R3)/R1+1 (the gain for this circuit = 101), then passed through the unity-gain differantial amplifier and through the gained OPAMP circuit, and finally transferred to the output. Second (bottom) is the one that is used to give AC and DC signals to motor, in which the input signal comes from the signal generator (Figure 8.5), then is transferred into the unity-gain OPA544 circuit, and then plugged into the linear motor. By this way, DC voltage coming from the power supply can be converted to an AC voltage to vibrate the motor shaft linearly.

By means of the PCB circuit (Figure 8.1), an offset DC voltage can be supplied to fix the motor shaft in any point of the indicator screen, and then give a p-p AC voltage to move the motor shaft sinusoidally based on the Lorentz Force Law. At the same time, the signal coming from the coil can be observed on the osilloscope screen (Figure 8.6). This signal is amplified by 101 times the main signal through a differantial amplifier.

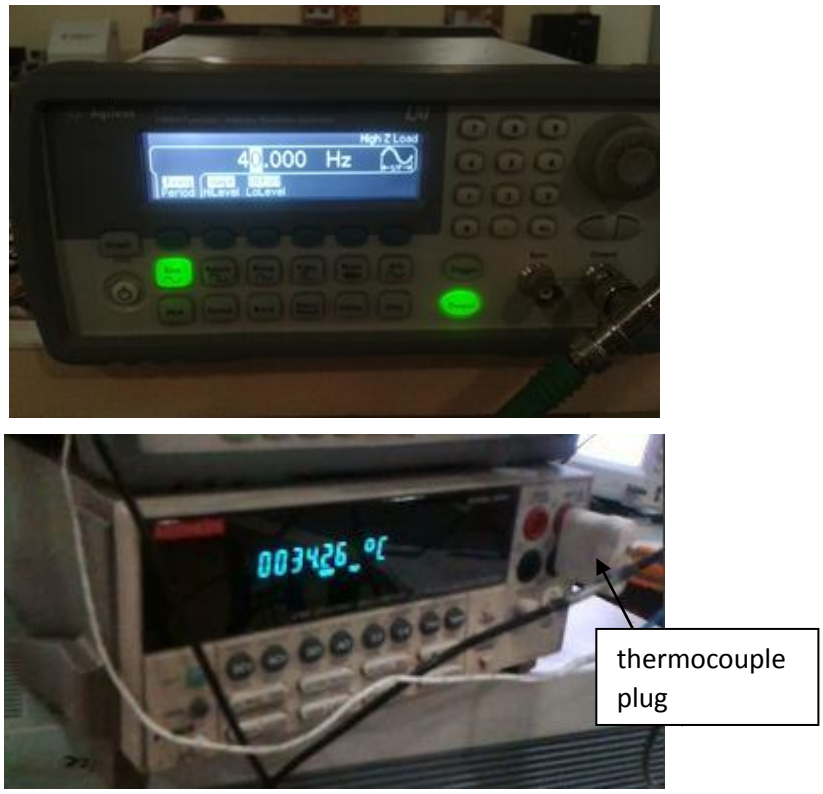

Figure 8.5: Signal generator(top) and multimeter (bottom)

Multimeter was used here to detect the temperature change by the thermocouple attached to the motor coil.

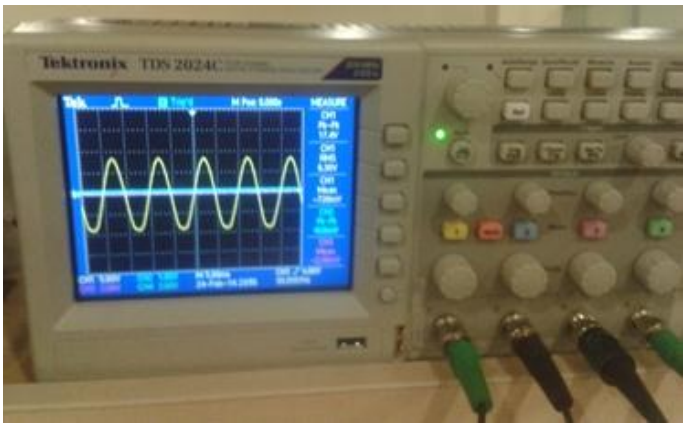

Figure 8.6 : Oscilloscope

8.2. TEST RESULTS

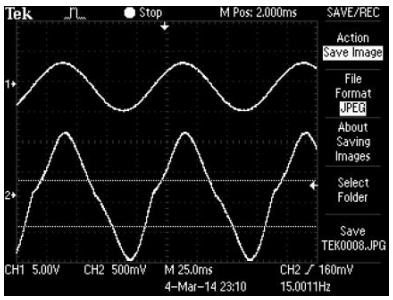

10 Hz
±5 V p-p

There is a friction based deviation from sinusoidal motion because of low speed and high amplitude.

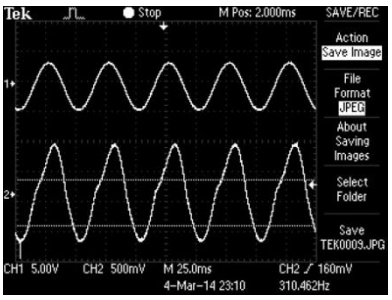

20 Hz
±5 V p-p

There is a friction based deviation of 10 Hz because of the same reason.

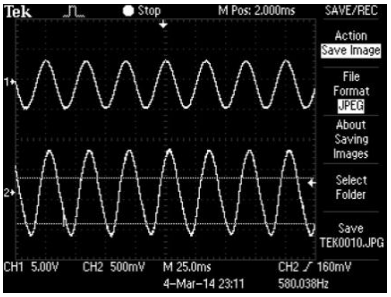

30 Hz
±5 V p-p
Nearly sinusoidal motion due to less friction because of higher speed and less amplitude.

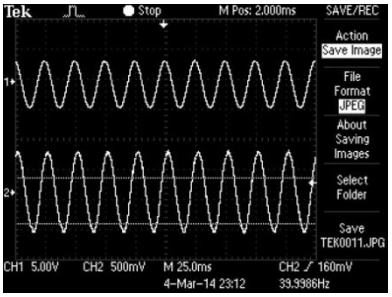

40 Hz
±5 V p-p
Nearly sinusoidal motion due to less friction because of higher speed and less amplitude.

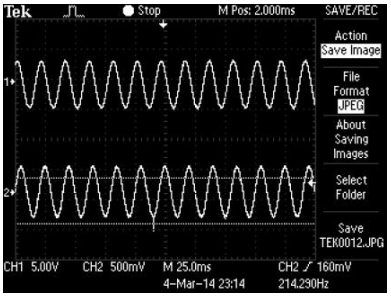

50 Hz

±5 V p-p

Nearly accurate sinusoidal motion

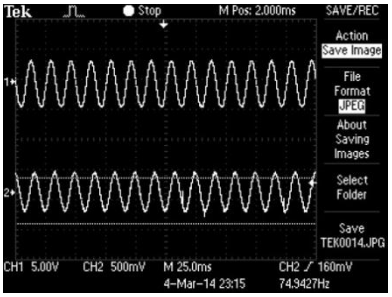

60 Hz

±5 V p-p

Nearly accurate sinusoidal motion

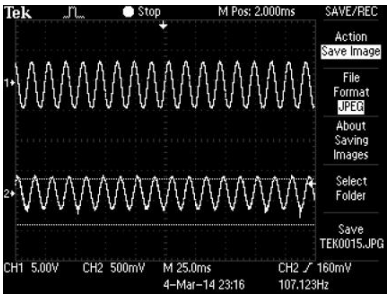

70 Hz

±5 V p-p

Nearly accurate sinusoidal motion

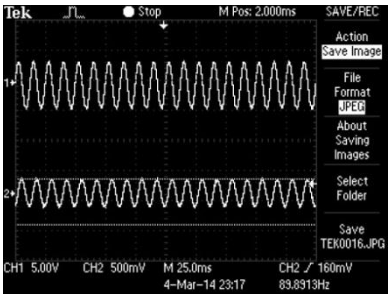

80 Hz

±5 V p-p

Nearly accurate sinusoidal motion

Figure 8.7: Sinusoidal motion testing with different frequencies.

In Figure 8.7, top wave comes from the motor driver signal that is applied to the motor to move the shaft. Bottom wave comes from the coil which is used to detect how close the motion is to sinusoidal motion. Each test took almost 10 minutes but there was no disruption at the wave during the time. Low frequencies, especially 10 Hz and 20 Hz show disruption because friction becomes very effective at low speeds. Hovewer, as high speeds are reached, friction becomes less effective. This is because sliding materials such as teflon and rulon guidings are still unused. After a short period, they will be involved in the sliding process.

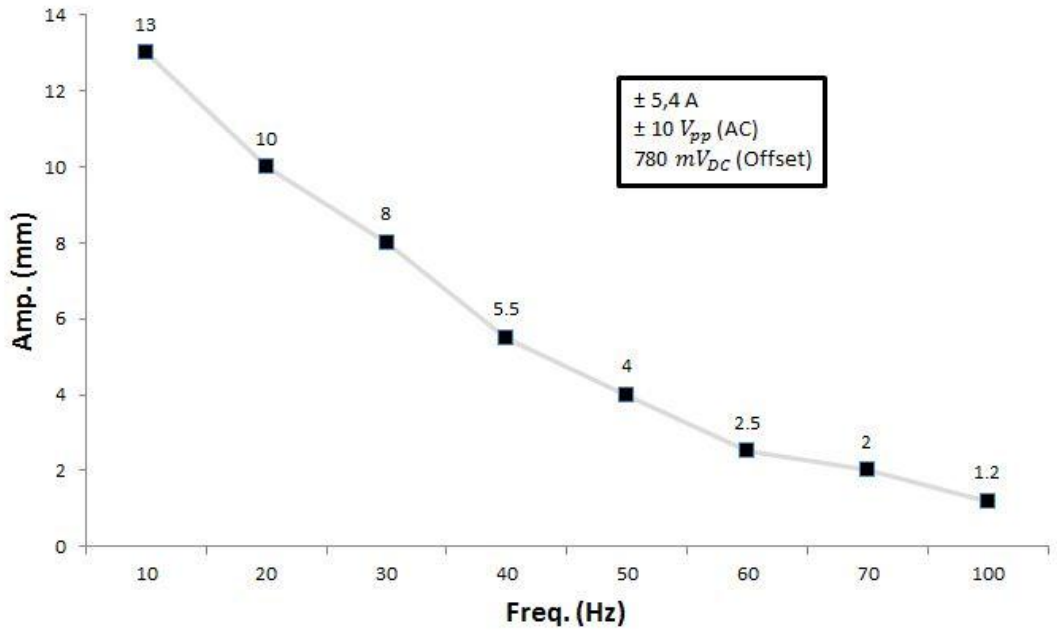

Figure 8.8: Amplitude vs. Frequency at ±10 V p-p, 5.4 A, 780 mV offset DC Voltage

The above graph is partly coherent with theoretical descriptions. If the ability of the circuits to provide any voltage is high enough, very high values might be reachable. Fortunately, these frequency and amplitude values are adequate to execute any VSM measurement, and that will also be enough to reach the sensitivity of 10^{-5} emu or higher.

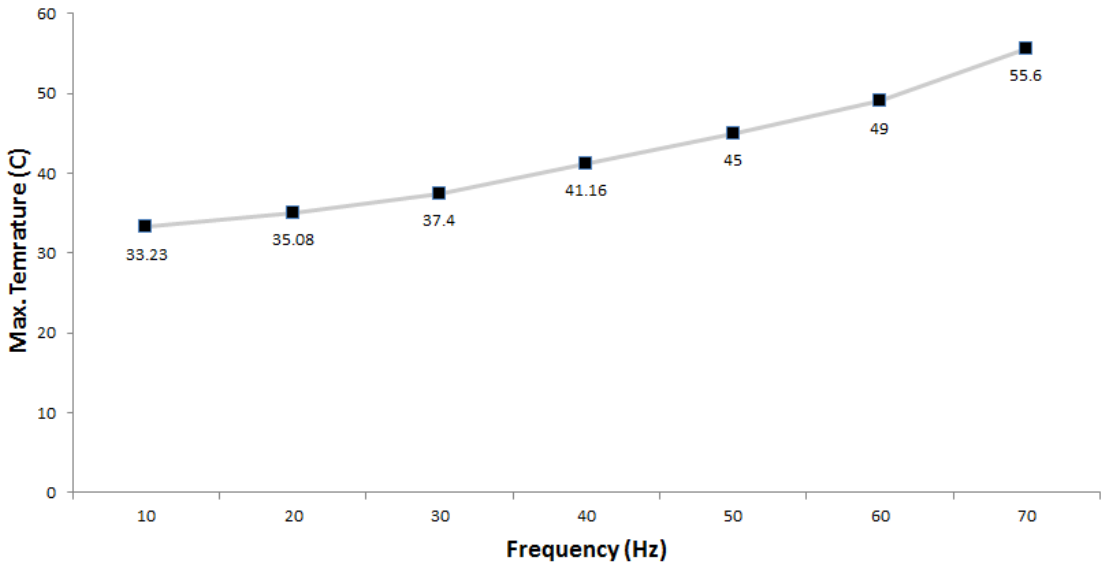

Figure 8.9: Max. Temperature vs. Frequency at $6{,}4 \times 10^{-4}$ mBar Vacuum condition after 6 minutes.

The test in Figure 8.9 is conducted at ±10 V p-p, 5.4 A, and 780 mV offset DC voltage. Actually, these temperature values are measured at the motor coil, and are not the ambient temperatures in the motor. These measurements were taken by a termocouple attached on the coil. Therefore, during testing, any reduction in amplitude is not visible which proves that there are no termal effects on the motor magnets. Also, the aluminum structure supplies a high thermal isolation for the motor coil.

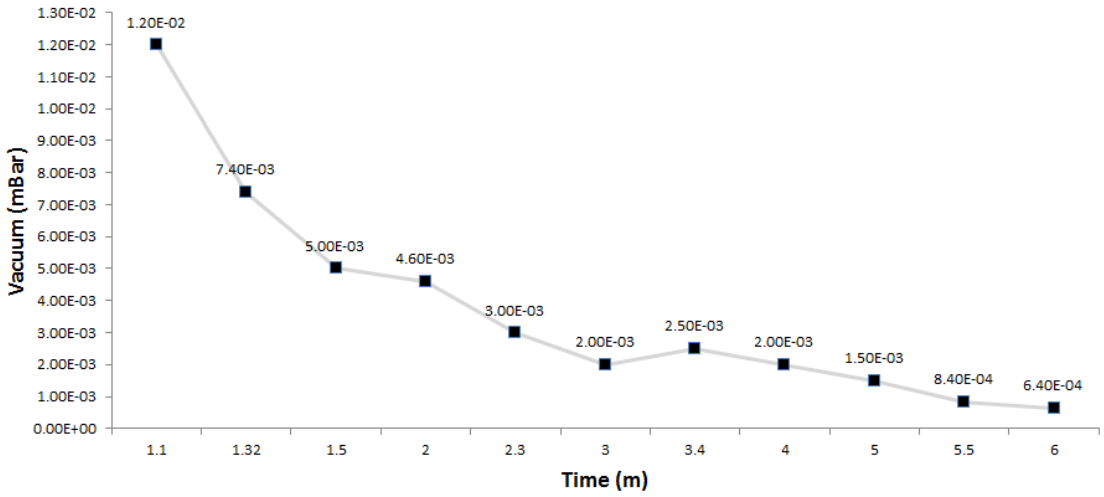

Figure 8.10: Vacuum vs. Time graph

For Vacuum testing, a Pfeiffer turbo & mechanical vacuum pump was used as shown in Figure 8.11. Figure 8.10 illustrates that in 6 minutes, ideal vacuum conditions for the VSM measurement is reached at the normal operating conditions of the motor.

Figure 8.11: Pfeiffer turbo & mechanical combo vacuum pump.

Moreover, sample centering enables us to center the sample in the middle of pick-up coils and electromagnets through offset DC voltage, 780 mV. Motor can locate the sample at any point in stroke line during vibration any specific frequency at the same time, which provides sample to find best location in the pick-up coil automatically so sensitivity of the measurement can be very high in this way.

Integrating the encoder with motor system, feedback is going to support the motion. Therefore, it prevents any errors in sample centering but this thesis study exclude sample centering process during VSM measurement.

CHAPTER 9

CONCLUSION

In the light of previous studies on VSM sample drives, particularly, considering previously manufactured linear motor types and their coherence to VSM, a novel motor-probe module has been designed and manufactured to increase measurement sensitivity. While doing this, most appropriate materials were selected. Especially, thermal properties and compatibility issues were considered. Unlike conventional linear motors, the new design fulfills the requirements to provide proper oscillation at high frequencies and motion with large amplitudes. In particular, the linear motor is supposed to move in sinusoidal motion. According to the theoretical background of VSM, the system can work properly only with a very accurate sinusoidal motion. The most crucial portion of the design was the magnet design. To succeed in this, a large number of analyses were performed through Maxwell electromagnetic analyses software. Types of different geometries were experimented. Since radially magnetized NdFeB strong magnets were not available in global markets, it was painful to make round-shaped structure. Also, radial ferrite magnets were not adequate to fulfill our demands.

After examining the hexagonal design, it was seen that this geometry led to very low magnetic strength on the motor coil. Quadrand design seemed to be convenient for our demands, but not only the field strength was low, but also the field distribution was not entirely homogeneous. Therefore, this design needed some modifications to improve its performance. Since one-piece magnets are very expensive and not available in local markets, one-piece large magnets were attempted to be created from small sized magnets. It was proved by the results of analyses that the magnets built from small-sized magnets have approximately the same values with

that of large magnets. That means the iron yoke structure gathered the magnetic stray field to make it homogeneous and exhibits the properties of a one-piece magnet. When magnet aligning of conventional linear motors was employed, it was seen that cogging error occurred in the analysis. This is not acceptable for VSM measurements with great sensitivity. In order to avoid cogging along the motor coil motion, long rod magnets were utilized. Even though, the design with three-magnets back to back had the same magnetic features with two-magnet design, the design with only one-magnet lacked some of these features. For both reducing expenses and weight, 2-magnet was preferred. In addition, it was observed that reducing the thickness of iron yoke provided us with a more homogeneous distribution, thus, the final design was determined accordingly.

Compatible materials were defined and the CAD design was performed in Solidworks. As the probe material, non-magnetic carbon fiber tube that has very low thermal expansion coefficient was used. Because of its light weight, total weight of the moving parts was highly reduced.

In performing the motion tests, Faraday's Magnetic Induction Law was utilized. For that, a magnet was placed on the sample rod and a pick-up coil was wired around the outer tube. PCB circuit that contains two combined circuits was prepared. While one of the circuits can give AC and DC current to move the motor, other can amplify the signal that comes from pick-up coil. Combined tests show that self-motion of the motor provides quite decent signal under AC current. Although, at lower frequencies, due to large amplitudes, it was exposed to friction and the signal was not properly sinusoidal, however, at high frequencies, friction was not that effective. Theoretical results may be higher than empirical results due to mounting defiency and friction because the all parts were mounted by hand. However, this reducing is not a problem because emprical results are enough to perform any VSM measurement.

The actual source of friction is sliding and rubbing parts. In course of time, the components will become more compatible with each other and the friction will disappear. So, it will be possible to observe sinusoidal motion at low frequencies, too.

Furthermore, maximum vacuum condition of 10^{-4} mBar was reached in 6 minutes. It means that the VSM measurement will be ready to run in 6 minutes considering the vacuum.

Heating graph shows that the maximum temperature is strongly dependent on the frequency. Also, increase in temperature has an effect on neither magnets nor the motor force. After long working times, no losses in force can be detected due to thermal isolation of the motor coil from other parts. A stroke capability of 53 mm provides centering of the sample during the measurement.

REFERENCES

[1] http://clxy.web.hebust.edu.cn/english/laboratory/largeequipments/18116.htm

[2] S R Hoont and S N M Willcock, *The design and operation of an automated double-crank vibrating sample magnetometer*, J. Phys. E: Sci. Instrum. 21 (1988) 772-785. Printed in the UK

[3] Rev. Sci. Instrum. 62 (3), March 1991

[4] E. E. Braggt and M. S. Seehra, Analysis *of induced EMF in vibrating-sample magnetometers*, 976 J. Phys. E: Sci. Instrum. 9 216

[5] Foner, S. "*Versatile and Sensitive Vibrating-Sample Magnetometer*". Rev. Sci. Instrum 30 (7):548–557)

[6] By Santhosh D.Shenoy, Studies *on the effect of high energy ball milling on thestructural, electrical and magnetic properties of some normal spinels in the ultrafine regime*, July 2004

[7] Ruediger Held, Stetson University, *Senior Research Project*, unpublished, Spring 1993

[8] Fausto Fiorillo, *Measurements of magnetic materials*, Metrologia 47 (2010) S114–S142

[9] Quantum Design, *VSM Option User's Manual, 1096-100*, Rev. B0 February 2011

[10] J. A. Gerber, W. L. Burmester, and D. J. Sellmyer, *Simple vibrating sample magnetometer,* Rev. Sci. Instrum. 53(5), May 1982

[11] A. niazi, P. poddar and A. k. rastogi, *A precision, low-cost vibrating sample magnetometer*, current science, vol. 79, no. 1, 10 july 2000

[12] Quantum Design, MPMS *SQUID VSM User's Manual*, 1500-100, Rev. C0 4-15 January 2009

[13] Rev. Sci. Instrum., Vol. 69, No. 9, September 1998

[14] Lake Shore Cryotronics, *Low Moment Measurements with a Vibrating Sample Magnetometer, The Performance of the Model 7400 VSM: Sensitivity*, Lake Shore Cryotronics, Inc.

[15] Lake Shore Cryotronics, *Low Moment Measurements with a Vibrating Sample Magnetometer, The Performance of the Model 7410 VSM: Sensitivity*, Lake Shore Cryotronics, Inc.

[16] Bowden, G. J., JPhys. E Sci. Instrum., 1972, 5, 1115–119

[17] Fausto Fiorillo, Isaak D. Mayergoyz, *Characterization and Measurement of Magnetic Materials*

[18] P J Flanderst and C D Graham Jr, Rep. Bog., *DC and low-frequency magnetic measuring techniques*, Phys. 56 (1993) 431-492. Printed in the UK

[19] E. O.samwel, T. bolhuis and J. c. lodder, review of scientific instruments volume 69, number 9 september 1998

[20] http://matxrz.net/vsm.html

[21] David Jiles, *Introduction to Magnetism and Magnetic Materials*, Chapman & Hall, 65-85, 135-153, 325-356 (1998)

[22] Quantum Design, *Mounting Samples Loosely Causes Moment Noise in VSM Measurements*, SVSM Application Note 1500-009

[23] Quantum Design MPMS *SQUID VSM User's Manual*, 1500-100, Rev. C0 January 2009

[24] Roland Grössinger, *Characterisation of hard magnetic materials,* journal of electrical engineering, vol 59. no 7/s, 2008, 15-20

[25] B. d. cullity, C. d. graham, introduction to magnetic materials second edition.

[26] Bill Black, et al in PCIM Power Electronics Systems, July 1993 *Voice Coil Actuators: Applications & Product Selection Guide*

[27] *Versatile and Sensitive Vibrating-Sample Magnetometer*, the review of scientific instruments, volume 30, number 7, May 4,1959

[28] Rev. Sci. Instrum. 62 (3), March 1991

[29] A. Niazi, P. Poddar and A. K. Rastogi, A *precision, low-cost vibrating sample magnetometer*, current science, vol. 79, no. 1, 10 july 2000

[30] Wesley Burgei, Michael J. Pechan, and Herbert Jaeger, A *simple vibrating sample magnetometer for use in a materials physics course*, Am. J. Phys. 71, August 2003

[31] P J Flanderst and C D Graham Jr, Rep. Bog, *DC and low-frequency magnetic measuring techniques,* Phys. 56 (1993) 431-492. Printed in the UK,

[32] S R Hoont and S N M Willcock, *The design and operation of an automated double-crank vibrating sample magnetometer*, J. Phys. E: Sci. Instrum. 21 (1988) 772-785. Printed in the UK)

[33] V. I. Nizhankovskii and L. B. Lugansky, *Vibrating sample magnetometer with a step motor,* Meas. Sci. Technol. 18 (2007) 1533–1537

[34] Johansson T and Nielsen K G 1976, *A low frequency vibrating sample magnetometer* J. Phys. E: Sci. Instrum. 9 852–4

[35] Creer; A. de sa and W. o'reilly K. M.J, New *vibrating sample magnetometers for use between 4 and l000°k.* sci. instrum., 1967, vol. 44

[36] http://www.atecorp.com/products/ling-dynamics-%28lds-test-and-measurement%29/v203.aspx

[37] Gerber, J.A, *Simple vibrating sample magnetometer,* Review of Scientific Instruments Volume:53, Issue: 5

[38] *Electromechanical Drive For Magnetometers* US 2003/0038627 A1, Feb.27,2003

[39] Quantum Design, *Application Note 1096-305*, Rev. B0 June 2010

[40] Ekta Gupta, Mr. RR Yadav, *PSpice Simulation of Vibrating Sample Magnetometer Circuitry,* International Journal of Engineering Research & Technology (IJERT), Vol. 2 Issue 9, September – 2013

[41] http://en.wikipedia.org/wiki/Linear_encoder